2015

Design and Implementation of a Passive Neurostimulator with Wireless Resonance-Coupled Power Delivery and Demonstration on Frog Sciatic Nerve and Gastrocnemius Muscle

Jose Aquiles Parodi Amaya
Louisiana State University and Agricultural and Mechanical College, jparod1@lsu.edu

DESIGN AND IMPLEMENTATION OF A PASSIVE NEUROSTIMULATOR WITH WIRELESS RESONANCE-COUPLED POWER DELIVERY AND DEMONSTRATION ON FROG SCIATIC NERVE AND GASTROCNEMIUS MUSCLE

A Thesis

Submitted to the Graduate Faculty of the
Louisiana State University and
Agricultural and Mechanical College
in partial fulfillment of
the requirements for the degree of
Master of Science in Electrical Engineering

in

The Division of Electrical Engineering and Computer Science

by
José Aquiles Parodi Amaya
B.S., Louisiana State University, 2013
May 2015

ACKNOWLEDGEMENTS

I would like to thank God for allowing to complete this Master's thesis, and enabling me to thrive after long days and nights of work. I would also like to acknowledge my parents since it is their efforts, teachings, and mentorship that have given me the ability to study abroad.

A warm thank-you to my professors that have enlightened me throughout my career. A special acknowledgement and thanks to Dr. Jin-Woo Choi for mentoring my project and for the encouragement to tackle hard problems in multidisciplinary fields.

Warm regards go out to my committee members: Dr. Jin-Woo Choi, Dr. Kidong Park, and Dr. Daniel Hayes. Their classes have greatly helped with carrying out this project.

Special thanks go out to all the colleagues in the lab, who make great company during long work days.

TABLE OF CONTENTS

LIST OF TABLES

LIST OF FIGURES

ABSTRACT

The thesis presented has four goals: to perform a comprehensive literature review on current neurostimulator technology; to outline the current issues with the state-of-the-art; to provide a neurostimulator design that solves these issues, and to characterize the design and demonstrate its neurostimulation features. The literature review describes the physiology of a neuron, and then proceeds to outline neural interfaces and neurostimulators. The neurostimulator design process is then outlined and current requirements in the field are described. The novel neurostimulator circuit that implements a solution that has wireless capability, passive control, and small size is outlined and characterized. The circuit is demonstrated to operate wirelessly with a resonance-coupled multi-channel implementation, and is shown powering LEDs. The circuit was then fabricated in a miniature implementation which utilized a 10 x 20 x 3 mm^3 antenna, and occupied a volume approximating 1 cm^3. This miniature circuit is used to stimulate frog sciatic nerve and gastrocnemius muscle *in vitro*. These demonstrations and characterization show the device is capable of neurostimulation, can operate wirelessly, is controlled passively, and can be implemented in a small size, thus solving the aforementioned neurostimulator requirements. Further work in this area is focused on developing an extensive characterization of the device and the wireless power delivery system, optimizing the circuit design, and performing *in vivo* experiments with restoration of motor control in injured animals. This device shows promise to provide a comprehensive solution to many application-specific problems in neurostimulation, and be a modular addition to larger neural interface systems.

CHAPTER 1. INTRODUCTION

1.1. Purpose of Thesis

The purpose of this thesis is to discuss the current neurostimulator state-of-the-art and propose a solution to problems found in this technology. The circuit proposed demonstrates a suitable concept for a neurostimulation device that can solve several of the current issues with the technology. The design was characterized, and its wireless, miniaturization, and neurostimulator capabilities were successfully demonstrated.

This thesis can be used as reference for a comprehensive neurostimulator design review by other individuals and serves to highlight the multidisciplinary aspect of neuroengineering. Further work is required to completely characterize the power delivery components, power requirements, and miniaturization design optimization.

1.2. Introduction and Motivation

Neural interfaces (NIs) are devices that allow communication with the nervous system remotely. Communication can occur in one or both of two directions, either stimulation into the nervous system, or recording from it. Traditionally, this information path has been dominated by electrical information measurement and electrical stimulus, which allow bi-directional communication [1]. The interfaces vary in type, location and purpose. Neural interfaces can be classified as intraneural or extraneural, be located in the peripheral or central nervous system, and be utilized as stimulators or receptors on both motor neurons and sensory neurons [1]. Types of NI vary from external electrocardiograms (ECG), electroencephalograms (EEG), and transcranial magnetic stimulation; to implantable microelectrode arrays (MEA), longitudinal intrafascicular electrodes (LIFE), electrochemical stimulators, and optogenetic neurotransmitter release [2]. Neurostimulators are devices dedicated to delivering stimuli to the nervous system. Microfluidics has also been used to allow chemical stimulation which focuses on the delivery of neurotransmitters to target nerve sites [3]. Advances in genetics have allowed the implantation of specific genomes that program the nerve cell to construct photoreceptors and place them in the cell wall [2], allowing light to stimulate the neuron by triggering neurotransmitter release.

The field of neural interfaces has changed dramatically over the past 30 years. Microelectrode arrays allowed direct recording of high-resolution information from the brain and nervous system[4, 5]. Neural interfaces were developed to enable the acquisition and analysis of neural signals. Research allowed more applications to be developed and a deeper understanding of the signals utilized by the nervous system to communicate with the human body and with itself. The importance of NIs became prevalent as systems that restored sensory and motor function to tetraplegic and paraplegic humans were developed, and is evidenced by the increase in publications and presentations related to NIs in current neuroscientific journals and conferences [6]. The benefits of research in this field can be seen in the ability to help people with debilitating sensory and motor impairments better interact with their environment, and give them a better

quality of life. Benefits can also be seen as technology is developed that allows humans to move past their bodies and create a different connection between the world and their brains [6]. NI technology has changed from rudimentary signal probe devices that measured and recorded streams of signals into complex sensitive electrode arrays that feed large amounts of data into computer systems that are capable of processing it to extract valuable neuronal information from the host. A practical example of this technology are closed-loop systems that enable humans with amputated arms to control a wearable robotic arm that allows them to feed themselves and interact with their environment [7]. Closed-loop NIs are comprised of a feed-back and feed-forward mechanism typically consisting of implantable electrodes that connect to a processing unit through wires which receives electrical signals from and delivers electrical stimulation to the nerve through the same pathway.

There are many neural interface devices such as the electroencephalogram (EEG) and electrocardiogram (ECG) that have been refined substantially since their conception and serve a variety of purposes. The technical issues of these devices have been extensively reviewed and resolved in many different ways. These devices also reside outside of the body. Modern neural interfaces are able to contact with the nerves themselves.

The rest of the well-known NIs are currently limited by issues which include: proper selection of peripheral nerve fibers to restore control and communication, specificity and understanding of neural information that is used for control and feedback, stability of the device itself, injury induced by the implant and undesired consequences [1], and longevity and power supply of chronic devices [8]. Typical NIs utilize the sensing electrode to record and stimulate at the same time, however, valuable improvements can be achieved by using a modular design for separate sensing and stimulation devices. It was found that an innovative solution was necessary due to these drawbacks in current neurostimulator technology. Further developments in neural interfaces and neurostimulators require a different approach that focuses on solving the current problems faced in the field.

Taking into account current neurostimulator limitations, a novel circuit is presented which solves problems of wireless capability, size, and passive operation and control in current neurostimulator state-of-the-art. The circuit operation was characterized in this work, and its wireless capability is verified. Preliminary *in vitro* experiments were performed on this circuit to verify its operation as a neurostimulator, and will be presented in this work.

1.3. Outline of Thesis

The objective of this thesis project is to design and implement a neurostimulator which could be small enough to be implanted in a distributed manner in various locations in the body.

The thesis is separated into five chapters. Each chapter discusses and summarizes what was presented. The first chapter outlines the motivation and purpose of the thesis.

Chapter 2 is a comprehensive literature review that begins with a physiological description of the neuron, proceeds to describe neural interfaces, and further describes current neurostimulators.

Chapter 3 presents and discusses current neurostimulator issues. A novel neurostimulator design is presented and characterized. The wireless capability of the device is also demonstrated with a multi-channel implementation that drives light emitting diodes (LEDs).

Chapter 4 shows work that was performed in order to miniaturize the design. This miniature implementation is then shown with a wireless power delivery system capable of eliciting compound action potentials in frog sciatic nerve, and causing muscle contractions in frog gastrocnemius muscle.

Chapter 5 concludes the thesis by summarizing the work that has been achieved and putting it in context with future work. Suggestions on how to improve the design and further work that is required is also discussed.

CHAPTER 2. LITERATURE REVIEW

2.1. The Neuron

The nervous system can be divided into the central nervous system (CNS) and the peripheral nervous system (PNS). The CNS is composed of the brain, brain stem, and spinal cord. The PNS is comprised mostly of branches of nerves that emanate from the spinal cord and traverse the body. These nerves are composed primarily of the axons of neurons. Neurons are the basic cell within the nervous system. They control the transmission of information within the nervous system. Neurons compose the brain which harbors memories, consciousness, thoughts, and thought processes. Neurons are also capable of transmitting primarily sensory and motor information to and from the brain. Current human understanding is incapable of fully elucidating the complex processes that occur constantly inside the brain, however, technology has enabled human beings to record and analyze signals traversing the nervous system. This technology is referred to as neural interface systems. Neural interfaces are a good prospect to shed light on the complex processes within the brain [9]. The main focus of the technology is to communicate with the brain.

The signals that originate from the brain and traverse through the nervous system to the peripheral muscles and the signals that originate from the sensory cells and traverse to the brain are a focus of neural interface studies. These are the simplest signals within the nervous system as they have a defined purpose easily understood from their target tissue or location, be it sensory or motor. The transmission mechanism that drives these communication pathways is separated into two types of signals, namely electrical signals for long pathways through neurons and chemical signals through short pathways between neurons [10]. The electrical signals are termed action potentials. Neural interfaces tap into these pathways and record signals, or stimulate these pathways to generate a signal to propagate through them. The fact that the action potentials within neurons propagate as electric current, and chemical signals are regulated through neurotransmitters allow researchers and scientists to develop mechanisms to emulate these signals and artificially initiate signal transmission within a neuron or nerve. The shape and biology of neurons are well-adapted to generating, processing, and propagating these signals.

The neuron is composed mainly of the cell body, dendrites, and axon (Figure 2.1). Dendrites are numerous extensions that receive signals from the axons of surrounding neurons, and relay information directly into the cell body of the neuron. The axon of a neuron is typically much longer than the cell body, and is involved in the transmission of an action potential from the cell body to a surrounding neurons through several branches that extend at the end of the axon. The length of the axon is covered with myelin sheaths which increase the speed at which the action potentials propagate. Action potentials propagate along unmyelinated axons, whereas they jump through myelin sheaths. This process is known as saltatory conduction. Myelin sheaths are separated by a space close to 1 μm wide known as the Nodes of Ranvier, and are electrically equivalent to an insulator with high resistance and low capacitance. The Node of Ranvier is rich in voltage-gated ion channels that propagate the action potential from one sheath to the next. The small space

between the branches of an axon and the dendrites of the next neuron is known as the synapse. The neuron receiving the signal is called the postsynaptic cell, and the neuron that transmits a signal is referred to as presynaptic. Chemical signaling is the mechanism that facilitates communication through the synapse. Neurotransmitter channels are activated when an action potential traverses the axon and reaches the outer branches. These channels release neurotransmitters into the synapse which activate surface proteins in the postsynaptic neuron. Signals in these pathways can be detected utilizing sensing equipment suited for electrical and chemical detection. It is also possible to stimulate these pathways through the introduction of electrical signals at the axon and neurotransmitters at the synapse to induce action potentials. The electrical characteristics of action potentials are interesting since they provide a close to "all or nothing" (or binary) mechanism for neurons to communicate. While this view has been held for quite some time now, there has been evidence showing that the waveform of action potentials varies, which allows for complex signals to be propagated [11]. In this document, we view action potentials as a binary event for simplicity.

The resting membrane potential for neurons in mammals is close to -60 mV. When the cell body is excited through excitatory post-synaptic potentials which raise the membrane potential to the threshold potential, typically about -10 mV, an action potential will be induced. The action potential event changes the membrane potential by about 70 mV with duration of 2-3 ms [11]. The stimulation that drives action potentials is termed the excitatory post-synaptic potential (EPSP) (Figure 2.2). EPSPs raise the membrane potential chemically through the flow of ions through ligand-gated ion channels triggered by excitatory neurotransmitters. EPSP is opposite to the inhibitory post-synaptic potential (IPSP) that is induced when inhibitory neurotransmitters stimulate the dendrites of a neuron. When sufficient EPSP events occur close together in time, the membrane potential rises over the threshold voltage and an action potential is induced. The signal then propagates through the axon and eventually reaches the axon branches where the chemical signaling mechanism is activated and the signal propagates through the synapse into surrounding dendrites through neurotransmitters, thus inducing an inhibitory or excitatory post-synaptic potential.

Closed-loop neural interface systems aim to record action potentials that traverse these pathways and relay that information to a processing unit which in turn delivers the appropriate stimulus to the target. Signals can be recorded in several locations in the body, including the brain, sensory neurons, motor neurons, the heart, and others. The processing unit can be anything from a reflex path, to the brain, to a computer chip. The stimulus can be delivered in several places as well, the most common being motor neurons or muscles. Depending on the application, neural interface systems can be broadly separated into two categories: intraneural and extraneural [7].

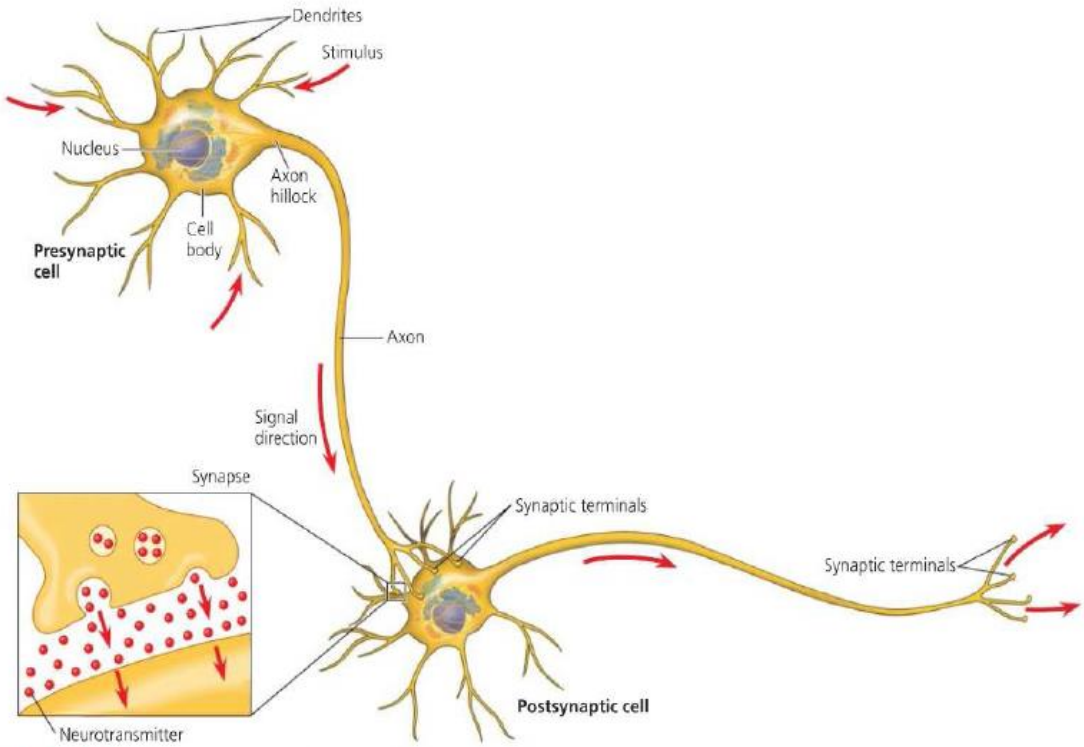

▲ Figure 48.4 Neuron structure and organization.

Figure 2.1. Neuron cell structure. The source is figure 48.4 from [10].

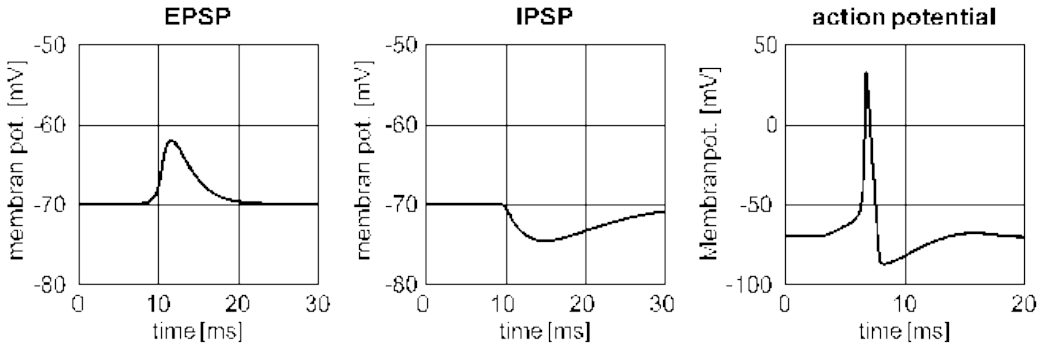

Figure 2.2. Typical EPSP, IPSP, and action potential waveforms [1].

2.2. Neural Interfaces

2.2.1 Overview of Neural Interfaces

Research focused on neural interfaces leads to the possibility of developing technology that will help people with damage to the nervous system. Treatments to the PNS sensory or motor neurons restores the interaction with their environment again [6]. Research has demonstrated the development of closed-loop prostheses that can be controlled and provide a mechanism to relay information back to their controller [12]. This type of research paves the way for developing a more clear understanding of the brain at the neuronal level. These advances in prosthetics and research have clear applications in clinical studies and important implications in the study of the brain in general. Neural interfaces that target the PNS are the focus of this section.

Neural interfaces are being developed to treat diseases or injury that has damaged the connection between the brain and body. Conditions such as stroke, tetraplegia, Lou Gehrig's disease, cerebral palsy, muscular dystrophy, limb amputations, and others can lead to the decrease in the ability for the brain to communicate with muscles properly while retaining the capabilities of generating the signals that would have enabled muscle control [6]. While the condition of the nervous system is different for nerve degeneration and damage and require different paradigms to develop a solution, neural interfaces provide a mechanism to relay the remaining brain messages to the appropriate muscular targets in order to restore function that was lost due to these conditions [13]. Brain signals are recorded and analyzed to provide control for technology that assists the individual in everyday tasks such as eating and dressing [12, 14]. They can also be used to drive functional electrical stimulation to control muscles no longer reachable through the neural pathway. Studies of monkeys with intact brains and humans with damage show that brain activity when muscle control is performed or imagined is similar [6]. The capability of the brain to create control signals even when there is nothing to control or the pathway has been damaged sheds light unto the importance of studying these signals and deriving useful information from them.

Neural interfaces have allowed specific action potential patterns from different places in the body to be extracted and analyzed [15]. This type of information has led to the development of several areas of neurological study such as: models for the encoding of action potentials, multiplexing of movement signals in distributed neural nets, comparison between action potentials and the summation of these signals, learning models and brain plasticity, the relationship between the brain and voluntary muscle movements along with brain control of machines separate from the body, and the recording of information from people with chronic diseases [6]. All of the mentioned fields have advanced extensively due to developments in NIs. Development in NIs does suffer from several technical difficulties that require specialized design and research, and implantable devices can fail over 40% of the time even when proper care has been taken during the implantation procedure [15].

The core difficulties of NI development reside in the fact that the body-machine gap has to be bridged. The obvious problems related to action potential coding and interpretation are stifled not by modern computational capacity, as was before, but by the inherent problems developed by installing a recording and stimulation system within a biological host. These issues arise from the biological response to foreign materials or tissue injury response. For the goal of reaching signals at the source, a surgical procedure must be performed. During any such procedure, tissue is damaged, and the body reacts depending on the type of damage and implant by initiating the wound healing process [16]. During the wound healing process, the implant or device are encapsulated in glial cells which have insulating properties. The cells impair the sensitivity of electric devices. The case is problematic at best for percutaneous systems that have wires running from the implanted device to the outside of the skin and into a processing unit. Percutaneous NIs also suffer from the possibility of infection and damage from movement [15]. For this reason, considerable effort is devoted into developing wireless, low-power, and high-bandwidth NIs [6]. Current technology helps alleviate the problem related to the body response through various coatings and drugs that inhibit the healing process. Another promising consideration when discussing the body's response is the mechanical properties of the implant. A recent study showed that when implants match the mechanical properties of the host, then the injury response is greatly reduced [17]. If a suitable solution to the biological response problem can be found, the main limitation to NIs resides in the location placement of the NI itself, and the communication with the user interface.

Neural interface technology is classified into two categories depending on where the sensing devices are placed with respect to nerve bundles. If the sensing device is placed on the surface of a nerve, it is extraneural. If sensing devices are placed within a nerve, they are considered intraneural [7]. Both types have their respective practical applications and will be discussed further in the following sections. In this thesis, devices that record or stimulate neurons will be collectively referred to as neural interfaces, regardless of whether the technology is utilized in a closed-loop fashion or not.

2.2.2 Extraneural Interfaces

Extraneural interfaces are mainly characterized by the fact that they do not penetrate the nerve when they are used to interface with the nervous system. Since the electrode itself is placed around a nerve which has few to many neurons within it, extraneural interfaces suffer from being unable to target single neurons [7]. Typical extraneural interfaces include the electrocardiogram (ECG) and electroencephalogram (EEG). In the ECG, the electrodes measure the summation of the action potentials that emanate from the heart. The EEG measures the voltages resulting from the action potentials of the brain detectable on the surface of the skull. These technologies have well-known clinical applications and have served to understand the underlying processes related to the natural heart pacemaker and brain signals [18, 19]. These systems, however, rely on electrodes being placed on the outside of the body, away from where action potentials are generated. In order to be able to record and stimulate specific nervous system pathways, it is necessary to place electrodes as close as possible to nerve fibers. They contrast with the electromyogram, which records

electrical signals from muscles. EEG, ECG and electromyograms are different from other neural interfaces that are located under the skin such as nerve cuff electrodes.

Nerve cuff electrodes manage to get close to the neurons by enveloping a nerve with electrodes and connecting these electrodes through wires to an external processing circuit. Thus, neural specificity is limited to the capability of placing the cuff electrodes at desired locations [1]. Typical nerve cuff designs are cylindrical, with electrodes and stimulation sites branching out perpendicular to the length of the cylinder with a central line that runs along the length of the cylinder [20]. Modern applications can utilize a flattened nerve cuff design with a rectangular cross-section which allows better contact between the individual neurons and electrodes. Nerve cuff electrodes currently still lack good specificity and thus are not prevalent components of NIs used for control of prostheses [7]. Nerve cuff electrodes do not damage or injure the nerve during implantation in any way when properly installed.

2.2.3 Intraneural Interfaces

Intraneural interfaces are ones in which the device penetrates the nerve and comes in contact with the neurons within. This characteristic makes intraneural interfaces capable of targeting a single neuron or a small group of neurons, which allows greater specificity of the signals recorded and a smaller stimulation signal to generate the desired effect [7]. Intraneural interfaces include microelectrode arrays (MEAs) [21], longitudinal intrafascicular electrodes (LIFEs) [22], sieve electrodes [23], microfluidic functional chemical stimulation and drug delivery [24], and optogenetic neurotransmitter release mechanisms [2].

MEAs consist of an array of electrodes placed on a semiconductor substrate. One well-known design is the Utah MEA[7]. MEAs have been evaluated in various systems with differing ports and implanting methods [25]. MEAs are suitable for sensing a collection of neurons at the same time since they cover an area of the nerve instead of a specific point. MEAs are suitable for recording and stimulation. Drawbacks of using MEAs is that currently their wired connections place unwanted stress on the device which may then move and injure the nerve that is targeted [7]. MEAs are still currently used with a wired connection to a separate processing unit [25].

LIFEs are characterized for being much longer than MEAs and consist of biocompatible devices which can be easily removed without further surgical procedures. Preliminary studies have shown promise in the prosthesis control field [7]. Technology arising from the combination of concepts from MEAs and LIFEs has been developed with advanced applications in NI systems [15]

Sieve electrodes consist of a sensor array being placed between two guidance channels in which the two severed ends of a nerve or neuron are placed. The field is then treated to promote neural growth, with the hope that the neuron will grow around the sensor array in the middle of the device [26]. Animal studies showed limited growth through the sensors, and applicability is further stifled by constant loss of nerve integrity and thus loss of nerve function [7]. LIFEs and sieve electrodes also suffer from the same drawbacks and limitations as MEAs related to unwanted stress being

applied to the nerve with possible damage incurred. All of the previous interfaces are typically connected to external processing circuits through wires that can induce unwanted stress on the nerves and pose risk of infection and unwanted tissue response.

Studies have attempted to develop electrodes accompanied by microchannels that are used to deliver drugs to treat neural damage and tissue response to the implanted devices with good characterization of the drug delivery mechanism [24]. Other microfluidic interfaces are designed to tap into the chemical signaling mechanism at the synapses. These interfaces have the advantage that they are not limited to the stimulation of nerves, but can also be adapted to be used to treat diseases that require local drug delivery and used to treat areas against tissue response which could inhibit the effectiveness of NI systems [3]. This project aims at providing a compact solution that will reduce the biological response from the wound healing process (by limiting device size) and allow wireless control to enable stimulation. The device should receive signals from an external processor and is designed to be used in a modular fashion as part of a larger neural interface system.

2.3. Neural Stimulator State-of-the-Art

Neurostimulators are devices dedicated to eliciting action potentials in targeted neurons. Recent advances in fields such as microelectromechanical systems (MEMS), bio-microelectromechanical systems (BioMEMS), optogenetics, biocompatibility, and wireless power transmission have paved the way for advanced neural interfaces to be developed. Current technology allows fully implantable designs to be feasible. The primary objective of a neural stimulator is to allow selective stimulation of specific nerve bundles for therapeutic or performance-enhancing purposes. There are three stimulation methods currently: electrical, chemical, and optogenetic.

Technology that enables neurostimulator ranges from transcutaneous electrical stimulation that targets large nerves (LIFE citation), microfluidics for the delivery of neurotransmitters to specific neural sites [17], to optogenetics which allows absolute targeting of individual neurons via excitation of photoreceptors produced by cells [27, 28]. Applications for neurostimulators include deep brain stimulation (DBS), vagus nerve stimulation (VNS), cochlear implants, cardiac pacemakers, chronic pain management, prostheses control, and computerized muscle control. Electric prescriptions are also an emerging field where bioelectronics devices are used to regulate the behavior of organs and organ systems in order to treat conditions. Current neurostimulators include the BION microstimulator [29], an ultrasound powered stimulator [30], a CMOS circuit-based stimulator [31], an integrated circuit stimulator [32], and capacitor-based stimulation systems [33, 34]. Table 2.1 summarizes the stimulation signal characteristics of all the discussed neurostimulators.

2.3.1 BION Microstimulator

The BION microstimulator has been in development for over 10 years now. It is a neural stimulator designed to be compact and easily implantable [29]. The general shape of it is cylindrical, having 2-3 mm diameter and about 20 mm length. This form factor was chosen specifically to make the

Table 2.1. Comparison of neurostimulator technology with respect to the proposed neurostimulation circuit.

Device	**Wvfm.**	**Power Src.**	**Power Freq.**	**Power Req'd**	**Stim. Delivered**	**Stim. BW**	**MC**	**Processing On-Chip**	**Neural Interface**	**Tissue Target**
[29]*	M	Battery, W	n/a	n/a	30 mA	1000	Y	Y	Electrode	Peripheral
[30]	DC	Ultrasound, W	1 MHz	10-150 mW/cm^2	1 mA	n/a	N	N	Electrode	Retinal
[31]*	B,A,C	Battery	n/a	224 µW	± 80 µA	200-10 k	Y	Y	Electrode	Retinal
[32]	B,A/S,C/I	Battery	n/a	n/a	n/a	n/a	Y	Y	Electrode	Retinal
[33]	M	Inductive, W	394 MHz	125 mW	0-150 mA	100	N	Y	Electrode	Peripheral
[34]	B,S,C	Battery	n/a	n/a	± 5 mA	n/a	Y	Y	Electrode	DBS
[35]	M	EM, W	.69-2.2 GHz	20.4 µW	80 mA	1	Y	N	LED	Optogenetic
[36]*	M	Inductive, W	n/a	n/a	1.4 mW/mm^2	10	Y	N	LED	Optogenetic
[37]	M	Battery, W	n/a	n/a	32 mW	1-20	Y	Y	LED	Optogenetic
This thesis	B,A,C/I	Resonant, W	>100 kHz	100 µW	40 nC	4 k	Y	N	Electrode	Peripheral,DBS,

Wvfm = waveform, M = monophasic, B = biphasic, A = asymmetric, S = symmetric, C = charge balanced, I = charge imbalanced, DC = direct current, MC = multichannel capability, EM = electromagnetic, W = wireless demonstration in cited document, DBS = deep brain stimulation, * Devices demonstrated with bi-directional technology.

device easier to implant though a syringe injection. It has gone through multiple design iterations. Originally, the BION circuitry was designed to operate in a completely wireless fashion with on-demand stimulation delivered through an external controller. Eventually, the design shifted towards utilizing a small battery that could power the device from anything between a few hours to a week of use, depending on how much it was utilized. The battery is designed to require 1-2 hours to charge fully.

The device is designed to allow several BION stimulators to be implanted in proximity. They have individually addressable circuitry that allows an external controller to select and program individual stimulators with different stimulation patterns. Latest BION devices also implement dedicated ASIC (application specific integrated circuits) chips with sensors that allow the device to record and transmit sensor information back to a controller. This feature enables bi-directional capabilities in the BION microstimulator [29].

Several clinical trials have been performed with the BION, including implanting in post-stroke patients for shoulder subluxation, muscle rehabilitation in patients with severe knee osteoarthritis, treatment of post-stroke hand contracture, treatment of foot drop, prevention of pressure ulcers, overactive bladder, refractory headaches, and gastroesophageal reflux disease [29].

2.3.2 An Ultrasound-Powered Neurostimulator

This device utilizes ultrasound transcutaneous energy transfer as its power source [30]. The operating principle of his power source is to deliver mechanical energy to piezoelectric materials to generate electricity. The design of this stimulator is simple, consisting of only 3 components: a diode, a capacitor, and a piezoelectric receiver. The device size was 1.3 mm in diameter, with 8 mm in length. The devices utilized a nerve cuff electrode as its means to interface with neural tissue, and this nerve cuff was specifically designed for rat nerves.

The device was shown to successfully stimulate rat nervous tissue, and elicit muscle contractions *in vivo.* The device managed to saturate the amount of energy delivered to the tissue until muscle contraction force could not be raised. Utilizing ultrasound as a means to deliver energy to low-power requirement devices is an area that has not been extensively explored. This specific type of power delivery is susceptible to beam direction and orientation of the receiver.

2.3.3 CMOS-Circuit Neurostimulator

The CMOS circuit presented in this paper was designed to be utilized as the implanted module (or device) in an external-internal system [31]. This architecture is based on two modules: one external control and data acquisition module, and one implanted module. The implanted device is typically powered by a battery. The implanted device presented in this case is an integrated circuit (IC) which has amplifier optimizations that reduce the IC size and increase its efficiency, two key parameters when designing neural interface chips. The IC includes a neural recording path, and a neurostimulation path. These two systems can be connected to the same electrodes and isolated

from each other, allowing the device to operate bi-directionally according to commands from the controller. The stimulation signal was designed as a square wave, but has capacitive latency associated with it. This issue prevents symmetric waveform generation. The device architecture is presented, and extensive simulations are shown, but no constructed device is shown. The simulations are promising, and further iterations and optimizations in different areas may lead to future low-power ICs with complete bi-directional capabilities.

2.3.4 16-Channel Neural Stimulator IC

A 16-channel neural stimulator is presented with applications in artificial retinal prostheses [32]. Like the previous described CMOS-circui, this device relies on an external control module. This system implements a digital to analog converter (DAC) at the external control module instead of implementing a DAC on-board every chip. This architecture manages to reduce device size by up to 51.8%. The 16 channels are utilized to drive "pixels," which are electrodes in an MEA which interface with the optic nerve to be able to cause 2D stimulation and generate artificial images.

A key design feature of this IC is that it allows great flexibility in terms of stimulation waveform generation. The circuit allows square wave, exponential cathodic, biphasic pulse trains, fast cathodic, sine, and fast anodic waveforms. Simulations have shown that different stimulation waveforms have different stimulation efficiencies [38]. This devices was successful at showing that neural stimulators can be successfully simplified by moving specific circuitry and applications to the control module.

2.3.5 Capacitor-Based Neurostimulators

Capacitor-based neurostimulation has particular advantages when compared with direct current and voltage controlled stimulation [34]. Stimulation is inherently safer due to the limited current available for discharge within a capacitor. Capacitor-based stimulation is also easier to control since charging the capacitor automatically imposes a limit to the charge stored without needing to implement a feedback loop. Capacitive-based stimulation does have a lower efficiency, but this is efficiency has been achieved at 77%, with 65% and 92% efficiency achieved in current controlled stimulation and voltage controlled stimulation systems [34].

In [34], a switched-capacitor stimulation (SCS) system is proposed. In this system, a power source charges a bank of capacitors which are selectively discharged to different electrodes through the use of multiplexers and demultiplexers. The system uses an integrated microcontroller and other control and safety circuitry. The microcontroller allowed for several stimulation parameters to be controlled, including stimulation voltage, current limit, stimulation pulse width, stimulation frequency, and electrode selection. The system was simulated and it has been implemented in other publications [36].

The proposed device in [33] assumes a simpler approach to SCS stimulation. In this device an ASIC is utilized to house a stimulation capacitor which stores the charge that will be delivered to

the target tissue. The capacitor limits the amount of charge that can be delivered to the tissue, thus providing a limit on the amount of energy delivered. In this manner, a microcontroller is not required. The device was implemented using a MEMS process and surface-mountable device (SMD) components.

2.4. Effect of Transmission Frequency on Tissue Absorption

Understanding the effect of the human body on the transmission of wireless energy is primordial when designing implantable wireless electronics. Energy loss in tissue affects transmitter and receiver antenna design. Receiver antennas are mostly affected since smaller devices approximating the wavelength of the transmitting frequency yield higher energy efficiency[39]. Choice of transmission frequency also affects the power amplification technology of the source, and component selection.

Modeling and simulations research have shown that there is substantial energy loss within the body at high frequencies [35, 39-41]. This is due to propagating fields showing a high energy absorption in tissue. Tissue interfaces such as air-skin, skin-fat, fat-muscle, and bone are sites where there is increased energy absorption[40]. Apparently, high frequency power transmission seems unfeasible inside the body however, [35] showed efficient power delivery at high frequencies between 690 MHz and 2.2 GHz. This increase in efficiency was due to the receiving antennas being smaller than the wavelength, and this allows power transfer to occur in the propagating fields region instead of near-field. Another paper by the same group estimated the optimal frequency at which wireless power delivery may be achieved for devices implanted in different body tissues[39]. Transmission frequency is a design parameter that falls outside the scope of this work, however it is an area that may be addressed in future work.

2.5. Summary

Chapter 2 begins with an overview of the neuron was presented to understand the biological target for neural interfaces. Neural interface technology was then presented with a distinction being made according to the interfacing location, be that inside or outside a nerve with electrodes, using microfluidics for neurotransmitter delivery, or using optogenetics to cause neurons to be susceptible to light. This distinction allows classifying neural interfaces into extraneural and intraneural. Neurostimulators are neural interfaces dedicated to stimulating nerves and the nervous system. A review on the state-of-the-art for neurostimulators was then presented. The advantages and disadvantages of nine devices are detailed and discussed. Capacitor-based neurostimulators were shown to be promising due to their safety features and easy control. Transmission frequency and how it affects energy absorption according to the tissue medium is mentioned as a factor affecting implantable devices however, it will not be addressed in this work.

CHAPTER 3. NEUROSTIMULATOR CIRCUIT DESIGN AND WIRELESS DEMONSTRATION

3.1. Introduction

Wireless neurostimulators are required in order to develop completely implantable, standalone neural interface technology. This technology is important due to the drawbacks faced by transcutaneous and battery powered neural interfaces. Transcutaneous applications suffer from complications such as infection, device translocation, and connections losing fidelity. Battery powered devices must be constantly recharged, or worse the battery must be replaced over time. This chapter focuses on discussing these problems and proposing a solution. The problems discussed focus on power consumption, size, and wireless capability in state-of-the-art neurostimulators. A novel neurostimulator design is proposed to solve these problems. The design is then characterized using benchtop components to verify it operates as designed. The characterization is focused on the output signal waveform. One of the advantages of the device is that it can operate utilizing AC power delivered wirelessly. A demonstration using resonance-coupled wireless power delivery is then shown to verify this feature. The circuit is demonstrated driving an LED, which is considered to require enough power so as to mimic successful nerve stimulation. In this chapter the neurostimulator design parameters are outlined, the requirements for a novel neurostimulator are described, the novel neurostimulator design is discussed and characterized, and a wireless demonstration is shown. The results are then summarized and discussed, along with suggestions to improve the experimental results.

3.2. Neurostimulator Design

3.2.1 Overview of Neurostimulator Design Parameters

In engineering terms, a neurostimulator is a pulse generator with various application-specific characteristics. There are several parameters that must be determined in order to design a neurostimulator. Parameters that have to be chosen for an implantable neurostimulator are according to [42]:

- Signal or pulse:
  - Waveform,
  - Amplitude,
  - Width or duration,
  - Stimulation frequency or pulse frequency,
- Load or tissue impedance,
- Power supply,
- Interface mechanism,
  - Electric,
  - Chemical,
  - Optogenetic,

- Packaging,
    - Encapsulation materials and coatings,
    - Dimensions,
    - Fabrication method.

Depending on the interface mechanism, the signal will have different requirements. In the case of microfluidic neurotransmitter delivery (chemical stimulation), a different set of specifications are required. Electrical and optogenetic stimulation share many characteristics, since optogenetics typically uses LEDs to stimulate photoreceptors in target neurons, and these are driven through electrical signals.

The tissue impedance is an important parameter in design since the output signal is largely affected by this impedance. There is variation in the reported resistance values of different nervous tissues and a study reported 100 Ω impedance in the vagus nerve of a rat[42]. Retinal tissue has reported values close to 10 kΩ [43]. 1 kΩ is chosen as a logarithmic middle ground between these values.

Packaging technology has advanced in recent years. The primordial goal has been to reduce the body's tissue injury response (TIR). This mechanism causes swelling and immune cells to rush to an injury site when tissue is disrupted. Injury occurs during implantation and surgery. Long-term TIR also involves the formation of giant cells which surround the foreign material and effectively isolate it from the rest of the body. These cells are particularly effective at isolating electricity, which is the reason for which many implants fail several weeks after implantation. Many advances have been made in order to reduce the tissue injury response by coating the implanted device in chemically biocompatible materials. A report has also been made that emphasizes that biocompatible materials are not related only to chemical properties, but rather the surface and mechanical properties of materials must also match the properties of the tissue surrounding the material. The report demonstrated breakthrough results with implant performance in rats which had neural interfaces implanted in their spinal cord[17]. The implants showed no rejection, and there was no deformation on the implant site beyond the damage caused by the implantation procedure. Further implantable devices must be biocompatible in these two areas for long-term stability to be guaranteed.

The output signal is the area of focus in this work. A proper design allows the capability to vary the signal duration, stimulation frequency, and charge delivered from device to device. The stimulation waveform has been shown to vary the efficiency of the stimulation, with symmetric triangular waves having the highest efficiency along with Gaussian waves [38]. Signal waveforms can be mono- or bi-phasic, and if bi-phasic they can be symmetric or asymmetric, and charge-balanced or imbalanced. Waveform phase determines whether the stimulation signal has a single polarity, or if the waveforms becomes both positive and negative during one stimulation cycle. If the waveform is also symmetric, this means that the cathode and anode phases are identical – akin to a full period of a sine wave. Charge-balancing requires that the charge delivered from the cathode and anode be identical. Charge balancing is also important to reduce probable injury caused to the target tissue [44]. The signal amplitude, in volts or amperes, is determined by the charge delivered to surpass the threshold voltage and cause an action potential in the target nerve.

n order to determine charge delivered during a stimulation cycle we need the current delivered during the stimulation:

$$\int_0^t I(t)dt \tag{1}$$

where t is the stimulation signal duration and $I(t)$ is the stimulation current. Once a waveform is selected, the signal or pulse must be designed to deliver a required amount of charge for electrical interfaces and light intensity for optogenetic interfaces. Charge delivered determines the chance that an action potential will be elicited at the target nerve tissue [45, 46]. The amount of charge required is 25 ± 17 nC for some nerve tissue types [46]. However, a correlation has been found between the amount of charge delivered to target tissue and tissue injury. The safe charge delivery limit for nerves have been found to be 1.38 μC [38]. Light intensity delivered for optogenetic interfaces varies according to the properties of the light source and area of tissue being illuminated.

The focus of the work in this thesis is to develop and characterize a neurostimulator circuit. The area of focus in this work is the signal or pulse generator circuit. This focus is due to the fact that the actual operating component of a neurostimulator is the signal generator. The rest of the device is subject to the constraints established by the neurostimulator, such as size and packaging, power delivery, and interface mechanism. The load impedance is determined by the target tissue, and is application-specific. The requirements of the neurostimulator and their rationale are discussed in the next section. Then, the design of the novel neurostimulator presented in this thesis is discussed.

3.3. Design and Characterization of Neurostimulator

3.3.1 Neurostimulator Requirements Overview

The review of state-of-the-art neurostimulators allows the outline of several problems that affect current neurostimulator development. The advantages of the separate designs can also be appreciated, and are now discussed. The BION microstimulator showed the advantage of using micro-sized components. This form-factor gives easy implantation methods through the use of a syringe. However, this design suffered from the lack of proper wireless power delivery methods, which is why later iterations implemented an on-board battery. This battery proves to be a substantial portion of the entire device size, and hampered the advantage of using micro-sized components. As with other neurostimulators, the BION microstimulator had to be programmed by a specialist once it was implanted, and the programming could not be easily changed by the user [29].

The ultrasound powered neurostimulator suffered from wireless directionality, since the device would not operate properly if it was misaligned from the ultrasound source [30]. The CMOS-circuit proposed as a front-end for retinal prostheses requires a battery which limits its implantability, and requires a data transfer scheme between the external and implanted modules [31]. The 16-channel IC showed similar features as the CMOS front-end, and it exemplified the advantages of having multichannel capabilities. This technology did not analyze the power

requirements, and it requires the use of a battery [32]. The capacitor-based neurostimulators have similar issues as presented.

Current neurostimulator applications such as DBS, VNS, pacemakers, chronic pain management, and electric prescriptions would benefit from a comprehensive solution that tackled the problems mentioned in current state-of-the-art. The following neurostimulator requirements are found for a neurostimulator in order to provide a comprehensive solution:

- Passive device: The device must not have an internal power supply, or contain any form of instruction or control processing.
- Small size: The device must have components that allow integrated circuit fabrication with few outside components. An ideal device will be capable of fitting in an area smaller than 1 square cm.
- Wireless Utilization: The device must be able to be utilized in a wireless manner.

A neurostimulator circuit is proposed and its operation and features are now discussed.

3.3.2 Neurostimulator Circuit

A novel neurostimulator circuit is shown in Figure 3.1[47]. It is divided into 3 distinct sections with different functionality. These sections are the stimulation circuit, a rectification and isolation circuit to provide power to the stimulation circuit, and a power delivery circuit which feeds into the rectification circuit. The stimulation circuit is designed as a modification of current capacitor-based stimulation circuits. The entire circuit is realized with a minimum of 7 passive components if the power delivery is a battery, and with 9 components if power delivery is wireless. The design components of the circuit are in the stimulation circuitry and the power delivery circuit.

The power delivery circuitry can vary according to the application of the neurostimulator. An LC resonance-coupled power delivery circuit is shown in Figure 3.1 for demonstration purposes. The rectification and isolation circuitry shown in green will provide appropriate power to the stimulation circuitry, regardless of whether AC or DC power is utilized. This is due to the rectification and isolation circuit which rectifies AC and passes DC with minimal distortion. This flexibility feature allows the device to work properly with various forms of power delivery circuits, including wireless power delivery system. The two transistors are required to properly isolate the two components of the stimulation circuitry. The stimulation circuitry shown in red is designed to have a specific on-off control scheme. The two RC circuits are chosen to have different time constants. When the device is initially powered, a signal will be delivered to the load as the two RC circuits are charged and settle to a low-power state. This low-power state is reached when both RC circuits are charged however, as the circuits charge there will be potential difference causing the aforementioned signal. Then, once the delivered power is cut-off, there will be another stimulation signal delivered as the two RC circuits discharge at different rates, leading to a potential difference across the load. This operating scheme is achieved utilizing only on-board passive devices, and gives a unique control mechanism that is dependent solely on the timing of

the input power. A graphical overview of the operation scheme is shown in Figure 3.2. The small number of passive components leads to the possibility of the device being implemented in a miniature scale. Simulations were performed on this circuit to verify the operational scheme.

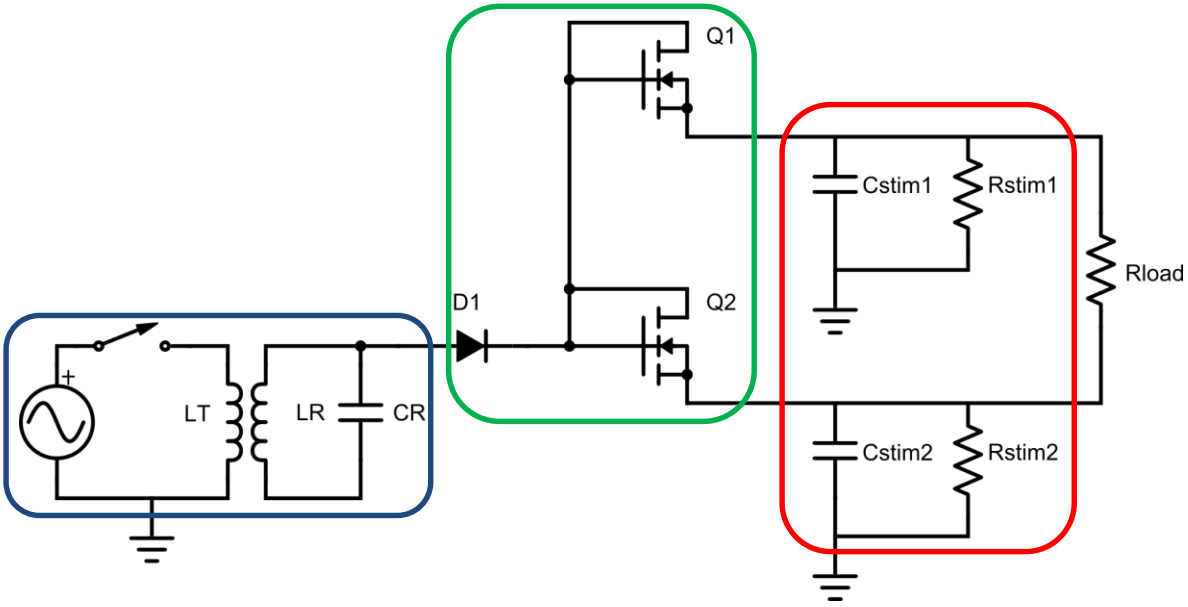

Figure 3.1. A proposed neurostimulation circuit. The blue section is the power delivery mechanism (shown as a resonance-coupled system here), the green is signal rectification, and the red is the stimulation delivery circuitry.

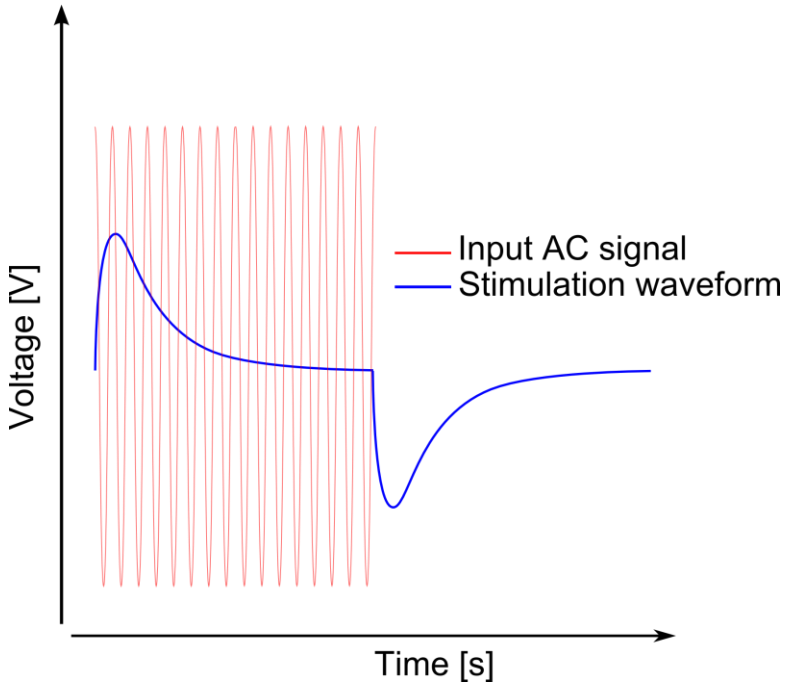

Figure 3.2. Overview of operational scheme for stimulation circuit.

3.3.3 Simulations

Simulations for the circuit (Figure 3.3) helped investigate the behavior of the device at several frequency ranges, capacitor values. Simulations were carried out in OrCAD 16.6 Lite version utilizing components built-in the standard OrCAD libraries. The resonant coupling system was not simulated since proper behavior of the triggering and stimulation systems must first be established. Simulations showed stimulation is about 10 ms per stimulus with the circuit in Figure 3.3 (Figure 3.4). Long-term simulations showed periodic fluctuations in the capacitors while they were charged (Figure 3.5). These fluctuations do not pose a problem to the circuit since they are minimal

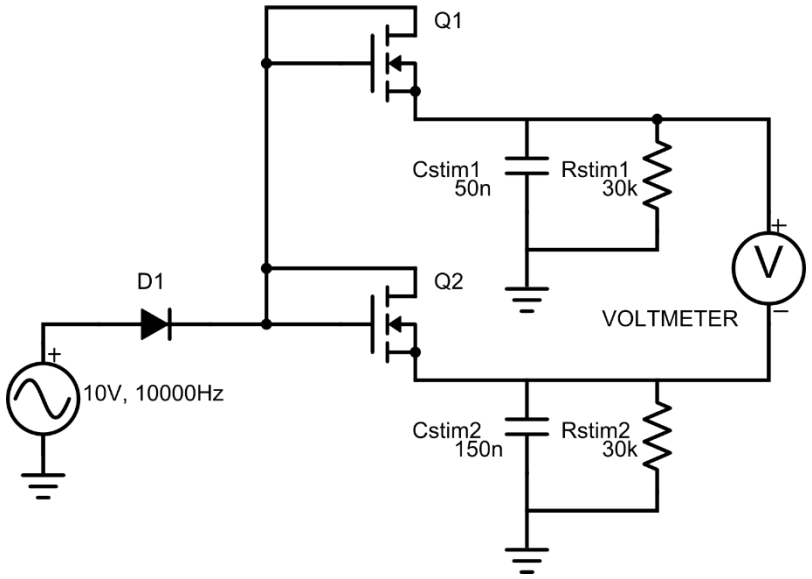

Figure 3.3. Circuit utilized in neurostimulator circuit simulations.

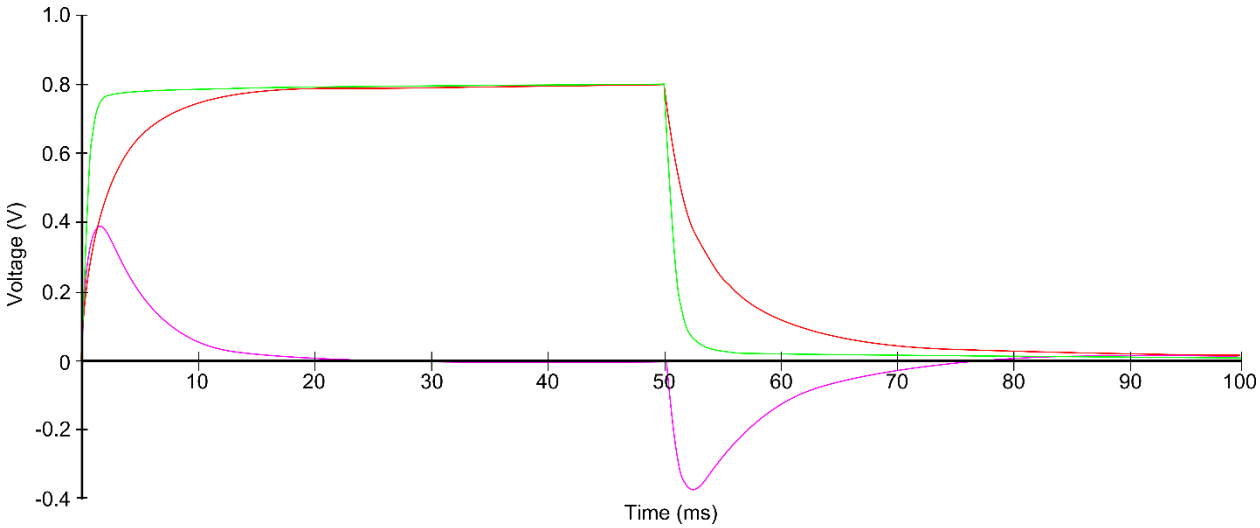

Figure 3.4. Stimulation results for the circuit in Figure 3.3. Green is the voltage at Cstim1, red is the voltage at Cstim2, and purple is the voltage difference between these two ports.

and the capacitors still have a stable charge. The circuit is passive since it does not process anything or contain memory, can be controlled by turning on and off the input AC signal, has components that can be built into an integrated circuit (IC), and the component count is small. The device meets all the requirements presented to improve neurostimulators.

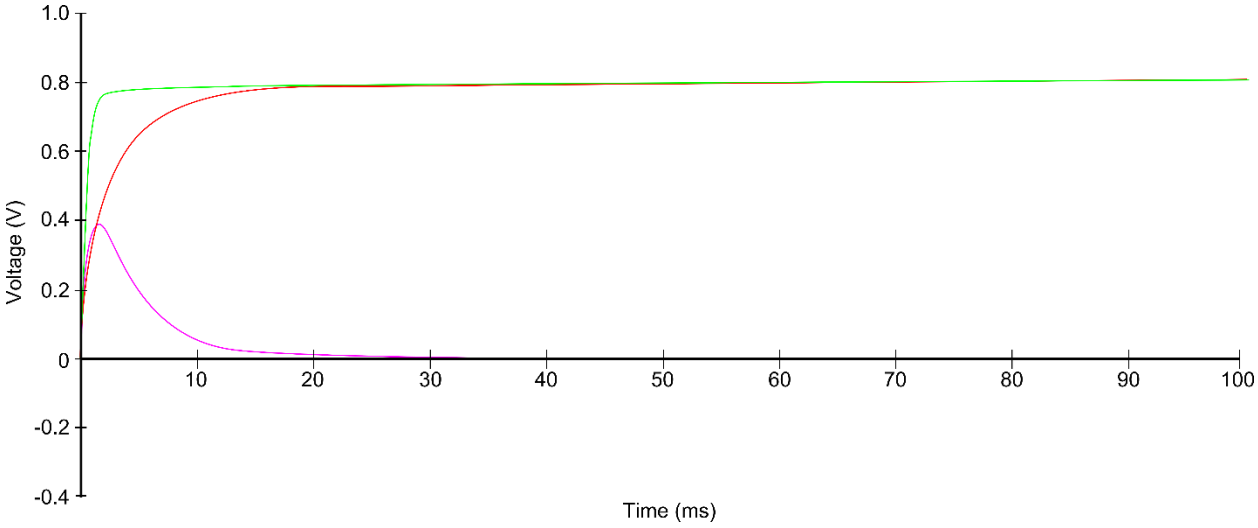

Figure 3.5. Long-term stability simulation while circuit is powered. Green is the voltage at Cstim1, red is the voltage at Cstim2, and purple is the voltage difference between these two ports.

3.3.4 Benchtop Characterization

The device was characterized in order to study the effect of varying the capacitance on the output signal. The circuit was assembled using standard axial and through-hole components to allow quick characterization. Characterization of the device was performed by fixing one of the capacitors, namely C_{stim1} at values ranging from 9 nF to 145 nF, and varying C_{stim2} between 9 nF and 990 nF for each iteration of C_{stim1}. The input power for this experiment was kept constant by utilizing a 20 kHz, 10 V_{pp} signal. A Keithley DMM 2110 was utilized for data collection. R_{stim1} and R_{stim2} were kept constant at 30 kΩ. The peak voltage and stimulation signal duration were recorded. Results are summarized in Figure 3.6. The time duration was largely governed by linear trends, and the stimulation signal amplitude varied with logarithmic trends. The lines of best fit equations for each case where C_{stim1} was fixed are displayed in Table 3.1.

The linear trend of the time duration is expected since the time constant is given by:

$$\tau = RC \tag{2}$$

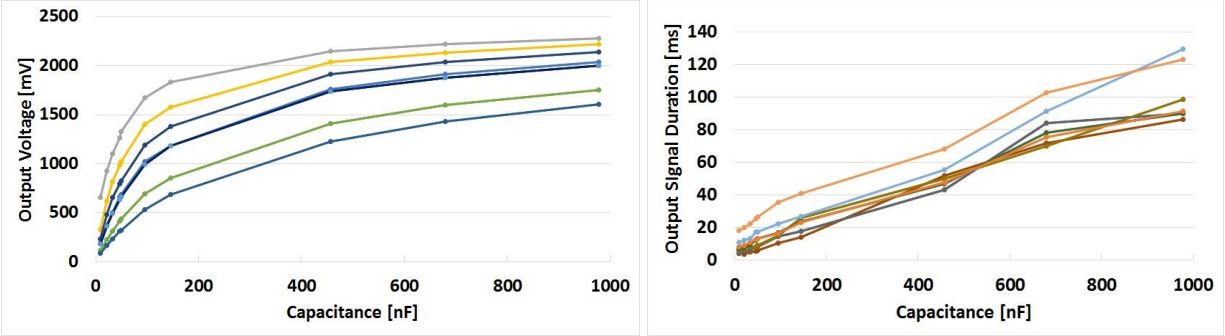

Figure 3.6. Variance of peak voltage and stimulation signal duration according to the variation of C_{stim2} between 9 – 990 nF when C_{stim1} is varied from 9 - 145 nF. The time duration showed a linear trend, and the stimulation voltage amplitude showed a logarithmic trend.

Table 3.1. Output signal duration and output voltage amplitude best-fit equations.

C_{stim1} (nF)	**Signal Duration trend line**	**Amplitude trend line**
9	0.0929x + 2.4911	364.53ln(x) - 118.63
21	0.0962x + 3.8671	425.67ln(x) - 625.41
33	0.0955x + 5.7456	435.25ln(x) - 817.43
47	0.09x + 7.7983	426.83ln(x) - 912.37
50	0.089x + 8.3954	421.15ln(x) - 905.38
95	0.1195x + 9.6193	379.16ln(x) - 946.36
145	0.1098x + 20.673	350.52ln(x) - 936.26

Since the stimulation signal time duration is determined by the charge and discharge rate of two RC circuits according to (2), it follows that it should be proportional to C. The stimulation signal amplitude has a similar reasoning, given that the voltage at a capacitor is given by:

$$V_{charging} = V_{input}(1 - e^{-\frac{t}{RC}}) \tag{3}$$

for a charging capacitor, and:

$$V_{discharging} = V_{input}e^{-\frac{t}{RC}} \tag{4}$$

for a discharging capacitor. Given these equations V_{output} can be shown to be for a discharging case:

$$V_{output} = V_{input}e^{-\frac{t}{R_{stim1}C_{stim1}}} - V_{input}e^{-\frac{t}{R_{stim2}C_{stim2}}} \tag{5}$$

As can be seen, as C_{stim2} is increased, τ increases for one of the RC circuits, causing it to discharge more slowly. The other RC circuit continues to discharge at the same rate. As C_{stim2} continues to be increased, the peak absolute potential difference across the output keeps increasing because the RC circuit that is not changed discharges at a much faster rate than the other circuit until the

dominant factor becomes the RC circuit that discharges more slowly. This trend is verified because the signal amplitude has an asymptote, which is an expression of:

$$V_{input} = V_{power} - (V_{f,diode} + V_{gs,transistor}) \quad (6)$$

Once the circuit was characterized and the trend equations described according to increasing capacitor values, the circuit was implemented with wireless power. This demonstration has the goal of validating the capability of the circuit to operate with wireless power.

3.4. Resonance-Coupled Multi-Channel Wireless Power Demonstration

The goal of this demonstration was to show the feasibility of operating the device using wireless power. For this case, the circuit was implemented using axial components. An LED was chosen as the load since it is easy to demonstrate successful operation by the LEDs turning on. A multi-channel implementation is possible by using different tuning capacitors for each LC circuit. 3 separate LEDs were lit using the same transmission antenna by changing the transmission frequency.

The power delivery methodology for the circuit is important since it determines the form factors in which the circuit can be utilized. Smaller, more efficient power delivery mechanisms will yield better overall systems, since they will be able to deliver stimulation in smaller spaces. Inductively coupled wireless require a strong coupling coefficient in the antennas, and require close proximity to work properly. Ultrasound power delivery seems promising, but it is largely an unexplored area, and there are several issues like implantation depth, effect on tissue on energy absorption, and tissue blocking which were not discussed in the aforementioned paper. Additionally, equipment is expensive.

Magnetic resonance-coupled power delivery has been a field of interest in recent years due to its easy implementation and adequate results. The only difference between inductive coupling and resonant coupling is that there is a capacitor placed in parallel with the receiving antenna. This forms an LC circuit that resonates at a given frequency. When this circuit is exposed to a varying magnetic field, it rings and efficiently absorbs energy at that frequency, while effectively attenuating energy emitted at different frequencies. Furthermore, inductive coupling can still provide power to the system. There are several factors that come into play when designing efficient resonant power delivery systems. The number of coils and the way they are coupled directly affects efficiency. In general, there are 2-coil magnetic resonant coupled power delivery mechanisms, which can be improved using 4-coils [48]. 2-coil magnetic resonant power delivery mechanisms involve a source, a driving LC circuit, a receiving LC circuit, and a load.

A 2-coil system was used to characterize the wireless capabilities of the novel neurostimulator.

3.4.1 Antenna Construction

The antennas fabricated for this experiment were designed to have good coupling coefficient, k, and intermediate size between 5 and 10 cm. The design was chosen at

- 20 turns using 28 American Wire Gauge (AWG) wire,
- 2-3 mm bundle thickness,
- Diameter of 6.5 cm.

The diameter was chosen due to the ease of using construction materials present in the lab. Four antennas were built with these parameters. The inductance of the antennas was tested to be 27 + 0.3 uH. Transmitting and receiving antennas were identical for this experiment to maximize power delivery. The 2-3 mm bundle thickness was chosen since this was the chosent thickness of miniaturized receiving antennas for our device in later iterations. Three different receiving antennas were tested with the same transmitting antennas, separately. Three different resonant

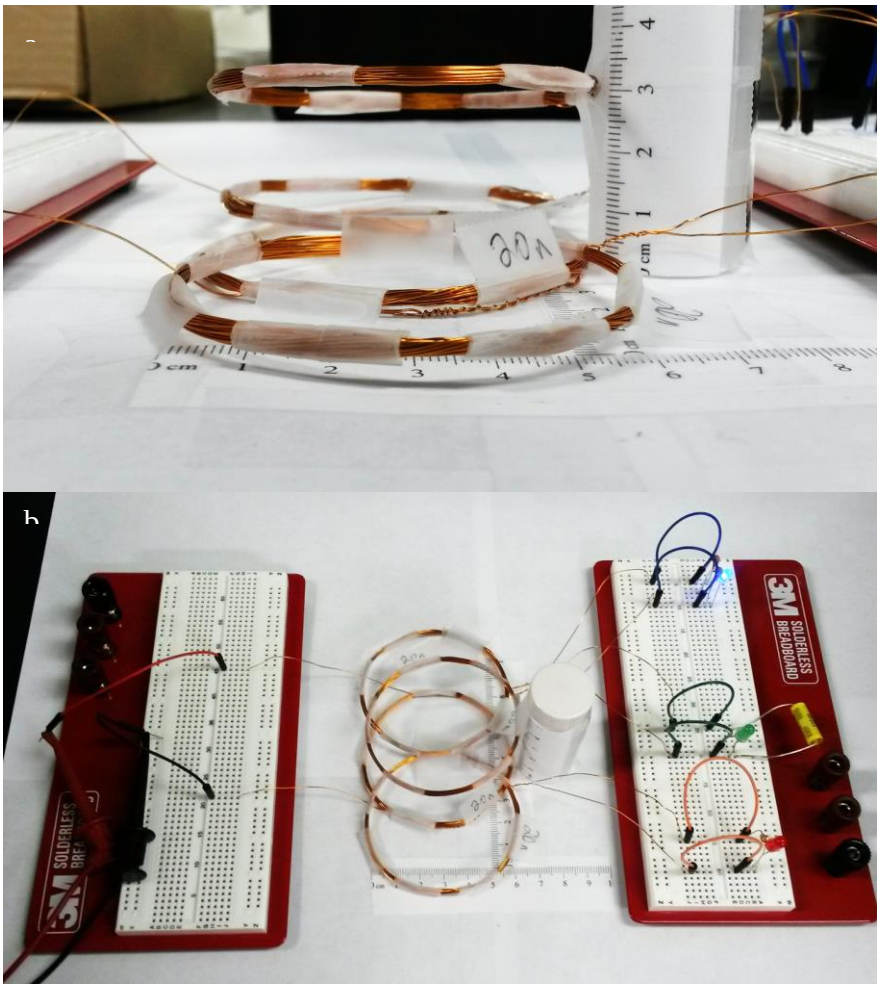

Figure 3.7. Resonant coupled power delivery circuit verification: (a) resonant coupled power antenna layout, (b) experimental setup with blue LED lit (top right).

capacitors were used, 490 pF, 9.9 nF, and 0.47 µF. These three circuits yield resonant frequencies of 680 kHz, 210 kHz, and 30 kHz, respectively. They were demonstrated driving three LEDs, blue, red, and green, respectively (Figure 3.7). The receiving antennas were located 3 cm away from the transmitting antenna axially, and then two of the receiving antennas were displaced 3 cm from the axis of the central receiving antenna. From the circuit design, it was determined that driving an LED had similar power requirements as the circuit. Thus, demonstrating a resonance-coupled antenna system driving an LED was considered a demonstration of sufficient power delivery to the stimulation circuitry.

3.4.2 Stimulation Circuit Driving LEDs

6.5 cm antennas were utilized. Resonant capacitors chosen were: 1.0 nF, 5.6 nF, and 10.1 nF. The resonant frequencies were then 621 kHz, 281 kHz, and 199 kHz, respectively. Blue LEDs with a V_{th} of 1.4 V were chosen for their high efficiency and brightness when fully turned on. The stimulation circuits were assembled using axial components with the following parameters:

- 1 Schottky Diode, V_{th} = 0.2 V (one circuit had a diode with V_{th} = 0.4 V), D_1,
- 2 2N7000 MOSFETs, V_{th} = 1 V, Q_1,
- 2 27 kΩ R_{stim},
- 1 10 nF C_{stim1},
- 1 220 µF C_{stim2},
- 1 68 Ω resistor.

The MOSFETs, diode, and R_{stim} are typical circuit components. The stimulation capacitors were chosen specifically to have a long stimulation signal time, allowing the LEDs to turn on for a long enough time to visualize them. The transmitting and receiving antennas were fixed to a block of packaging foam to maintain the transmission distance constant during the demonstration. The stimulation circuit was shown driving 3 LEDs independently of each other (Figure 3.8). A GW Instek AFG 2225 arbitrary function generator (AFG) was used to generate the transmission frequency signals. This AFG supplies 50 mA current at a maximum 10 V_{pp}. The central LED (corresponding to the central receiving antenna closest to the transmitting antenna) received more power than the adjacent 2 LEDs. The brightness difference between the 3 stimulation circuits emphasizes the power difference. The device was successfully demonstrated using wireless power, and shown in a multi-channel implementation with stimulator selection based on resonant frequency.

3.5. Summary and Discussion

The need for a novel neurostimulator was presented and discussed. The requirements for this neurostimulator were outlined by analyzing current state-of-the-art neurostimulators. The circuit for a novel neurostimulator was then presented and its operation was discussed. The characterization of the circuit was presented using benchtop components, and the relationship

between the results and the circuit components was shown. The circuit was designed to solve current neurostimulator issues related to component count, controllability, and wireless capability. The device was then demonstrated with a wireless resonance-coupled power delivery system. This system had the added advantage that resonant circuits could be tuned to show multi-channel control.

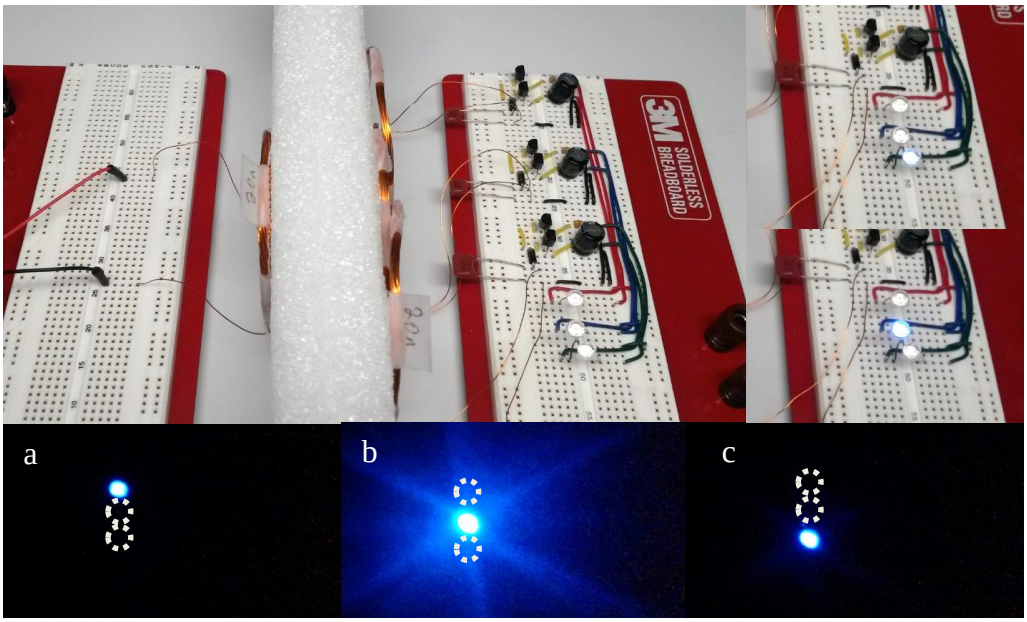

Figure 3.8. Stimulation circuit tested with resonant coupled power delivery: (a) top circuit lighting top LED; (b) middle circuit lighting middle LED, and (c) bottom circuit lighting bottom LED. The dotted circles show where the un-lit LEDs are located. Note the middle circuit shines brighter due to the receiving antenna being closer to the transmitting antenna.

The study presented in this chapter can be improved by providing optimized circuit analytical equations. The charging case for the output voltage has a different operational equation than does the discharging case. This is due to the fact that the input port during the charging case is a transistor, which acts as a current source when it is turned on. The circuit design is also an area of optimization. The diode in the rectifying may be removed in an optimized design, allowing lower power consumption with the same performance. Further work on this analytical solution is necessary. Further work to characterize the amount of charge delivered according to variation in the stimulation circuit design is also required. Additionally, the wireless power delivery system has not been optimized. Further characterization of the antennas, such as the Q-factor, coupling coefficient, and energy transmission efficiency are important to characterize in order to improve the current power delivery system. Accurate power analysis is also an area that can be developed, since this parameter will determine the size and shape of the power delivery system. Future work is suggested around these areas, as they will provide a more complete picture of the qualities of the circuit and the necessary design decisions that must be made for specific applications.

The demonstration of the proposed neurostimulation circuit operating with wireless power is a key demonstration for modern neurostimulation applications. The added multi-channel capability is also an important feature required in modern devices. The stimulation circuit was shown to be able to drive a different load than purely resistive loads, namely an LED. This result is of particular significance in the field of optogenetics, which is gaining increasing popularity, research, and applications. This section concludes the first goal of this thesis which is to present a novel solution for neurostimulators and characterize its operation. Further work was performed in order to verify the proposed circuit design operates as a neurostimulator, and can be properly assembled in a miniature implementation. This work is presented in the next chapter.

CHAPTER 4. STIMULATION OF FROG SCIATIC NERVE AND FROG GASTROCNEMIUS MUSCLE

4.1. Introduction

The goal of this chapter is to corroborate the design presented in the last chapter actually works as a neurostimulator, and show that it can be miniaturized. The fabrication process for the miniature implementation will be described. The outline of the experiment will be presented and the materials used will be discussed. Results of the experiments will then be presented. A discussion and conclusion will summarize the chapter. Improvements will be mentioned in order to add to the validity of the experiment.

Correct performance of the device to operate as a neurostimulator is fundamentally required. An *in vitro* or *in vivo* implementation is required to demonstrate the circuit functions properly. Additionally, the device cannot be large, use axial components, or use large antennas. This would not accurately reflect the intended application of the circuit. The goal of this experiment is thus to demonstrate a miniature implementation of the circuit powered wirelessly eliciting action potentials *in vitro.*

4.2. Wireless Device Miniaturization and Fabrication

4.2.1 Antenna Construction

The larger 6.5 cm antennas utilized for the wireless power demonstration are out of range for a sufficiently small device. Smaller receiving antennas were built for miniaturization testing purposes. They were oval in shape with the following parameters:

- 10 turns using 28 AWG wire,
- 2-3 mm bundle thickness,
- 10 x 20 mm dimensions.

These antennas showed good performance when coupled with a 6.5 cm antenna as the transmitting antenna. This antenna was constructed several times as the fabrication process was refined. The miniature antenna would be coated in nail polish enamel. The enamel gave the antenna rigidity to allow the manipulation of the antenna and soldering of components to it. This antenna was used for the miniature fabrication and neurostimulator validation experiment. Since the antenna determines the maximum size of the device, the circuit has to be implemented in a form factor that will fit inside the antenna. A miniature circuit implementation is discussed next.

4.2.2 Materials Selection

The miniaturization process begins with the selection of an adequate antenna. The miniature antenna constructed for this application was selected since it provided adequate space to fit a resonant capacitor and miniature circuit. The goal of the antenna is to harvest as much power

possible to deliver to the stimulation circuit. Given this fact, the antenna is then the largest component in a miniature implementation of the device. These antennas showed promise to deliver enough power to the stimulation circuitry from preliminary tests performed with 6.5 cm antennas as transmitters.

The rest of the device is miniaturized by choosing all SMD components in order to assemble the circuit in a small form factor. While the antenna is the largest component of the miniature system, the assembled circuit cannot exceed the antenna thickness of 3 mm. The smallest components that could be manipulated by hand were 0402 inch packaging case for the capacitors and resistors. For the MOSFETs and diode, an SMD with pins instead of contact pads was chosen since they were easier to manipulate by hand with little risk of shorting connections. The MOSFET and diode must also have a small V_{gs}/V_f to improve power efficiency. The list of materials for 1 miniature device for this experiment is as follows:

- 1 miniature antenna,
- 1 1SS367TPH3F Schottky Diode, $V_f = 0.23$ V,
- 2 Sl1012CR-T1-GE3 MOSFETs, $V_{th} = 0.4$ V,
- 2 ERJ-2RKF5102X 51 kΩ resistors, 0402 package,
- 1 C1005X5R1E334KBB 0.33 µF capacitor, 0402 package,
- 1 GRM155R71E473KA88 0.047 µF capacitor, 0402 package.

The device components before assembly can be pictured in Figure 4.1. The capacitors were chosen to deliver a moderate length signal 1-5 ms in duration, with approximately 280 nC of charge delivery with 1 V.

4.2.3 Fabrication Process

The circuit device size was an important consideration during the fabrication process. A PCB implementation would incur a considerable volume increase, even with a polyimide substrate. A layout was designed to optimize the circuit assembly and leave easy access to the power, ground, and electrode connections (Figure 4.2). For this layout, small wires <1 mm in length and components were soldered in direct contact. A custom fabrication process was developed in order to manipulate micro-sized devices.

Polymer oven-bake clay (Sculpey ORIGINAL Polyform) was utilized as a molding substrate to hold the SMD components in place during fabrication. This substrate is well-suited for this application due to the easy molding and de-molding process, and the high heat resistance. Additionally, the clay also works well as a heat-sink for excess heat to dissipate from components that are not being worked on.

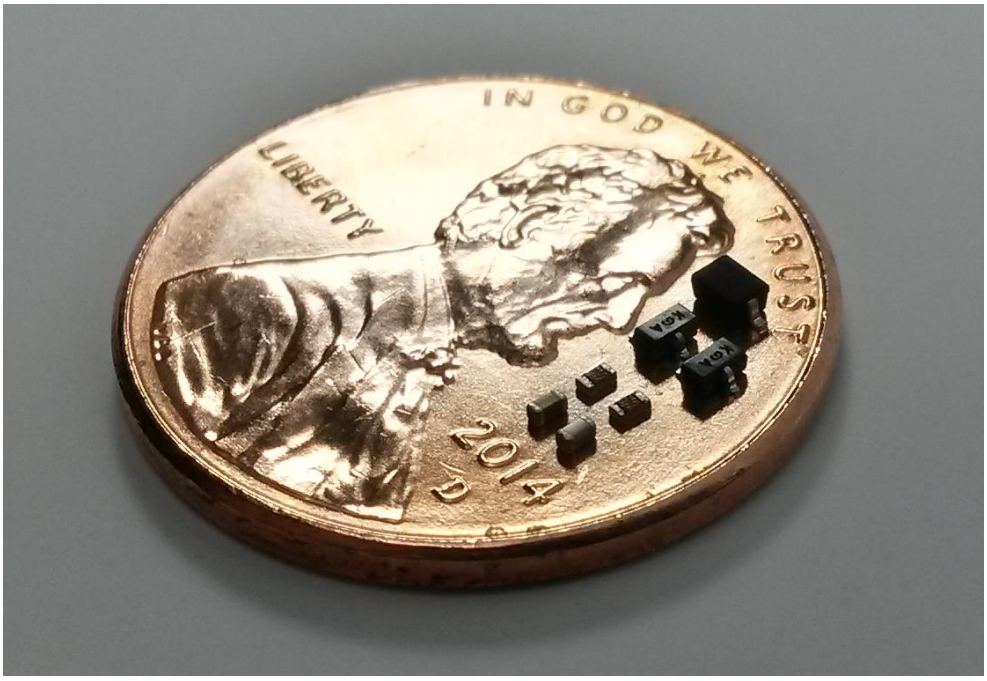

Figure 4.1. Circuit components for custom SMD fabrication.

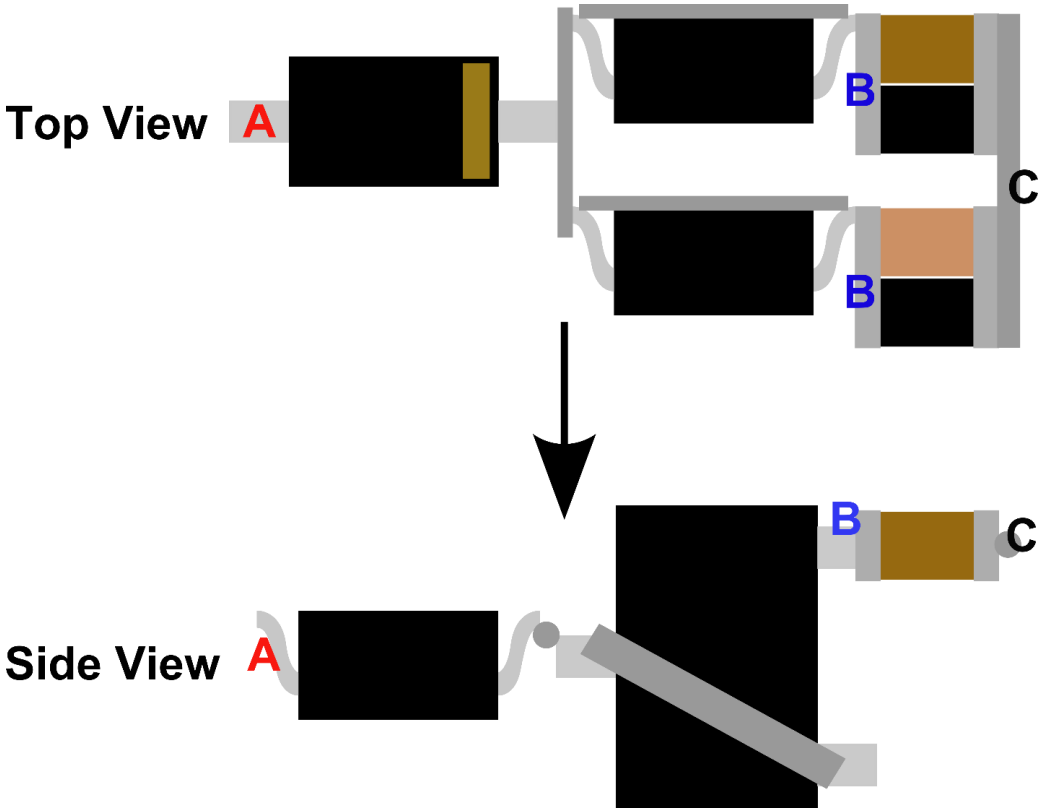

Figure 4.2. Miniature SMD layout: (a) input power port, (b) output electrode sites, (c) ground port.

The process begins by carving out a tiny clay cube approximately 5 mm^3. Then, the parts that will be soldered together are laid out in contact with one another on the clay substrate. Solder paste is then applied in the area that will be soldered. It is recommended that only one interconnection be formed at a time. As the final step, the clay is subjected to hot air from an SMD rework station set to 400 degrees F and low-medium air flow. The air flow is limited in order to prevent the air from moving the components while heating. The process is visualized in Figure 4.3 (make this one). The resulting assembled device is shown in Figure 4.4, and has dimensions 5 x 3 x 2 mm.

Following the circuit assembly, the miniature antenna is soldered to the resonant capacitor to add stability. 4 wires are soldered to the input, ground, and 2 electrodes of the circuit. The ground and input interconnections are then soldered to the cathode and anode of the antenna capacitor. The resultant device is shown in Figure 4.5. This device is considered the first miniature prototype and has approximately 1 cm^3 in volume. The tissue used in this experiment is discussed in the following section.

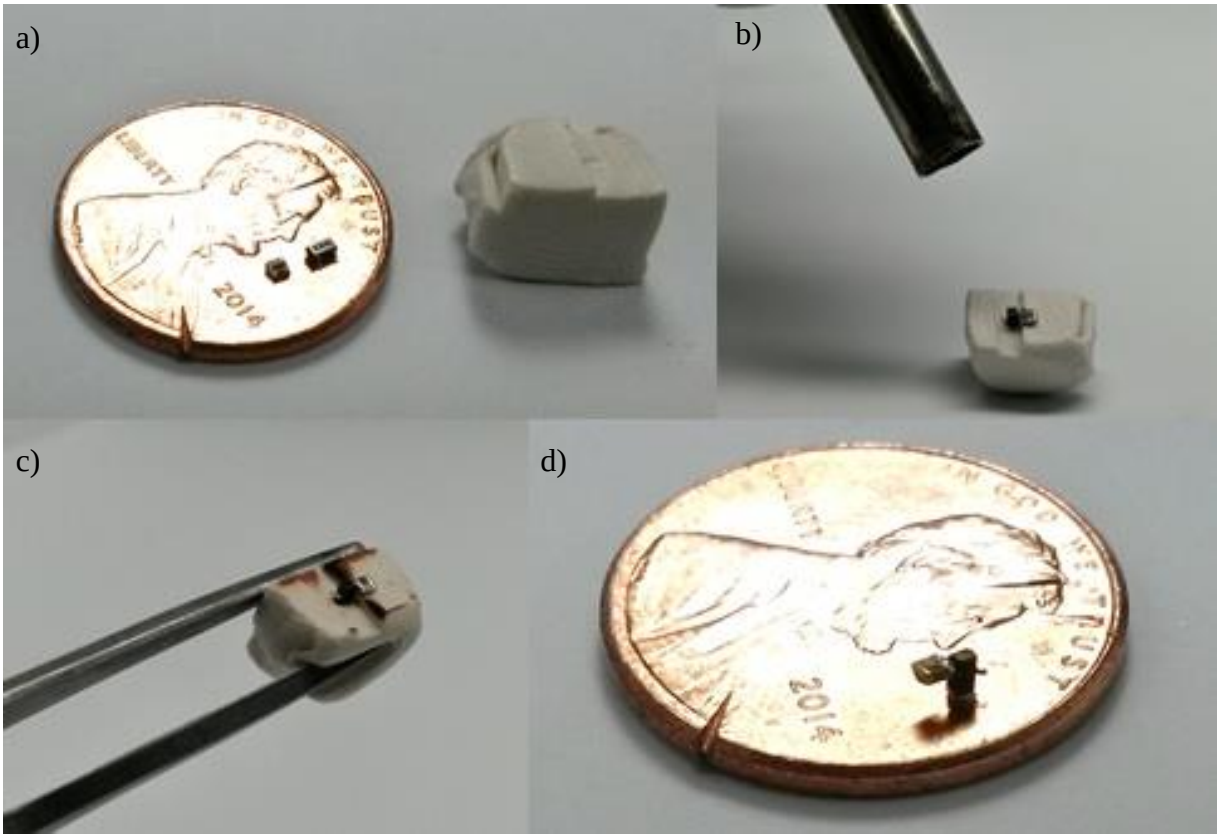

Figure 4.3. Custom fabrication process step utilizing clay substrate for SMD soldering, (a) components to solder and clay carved for support of 3D structure, (b) heating components laid out on clay with solder paste on interconnection, (c) components after soldering with clay showing minor shrinking, (d) a resulting structure.

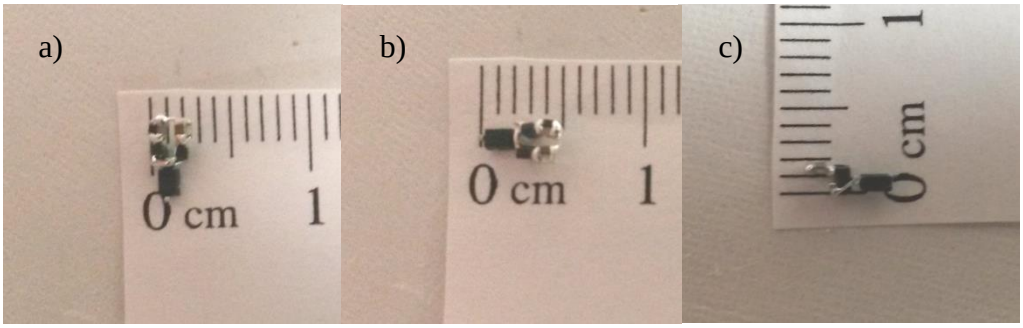

Figure 4.4. SMD device fabricated through process in Figure 4.3: (a) width 2.5 mm, (b) length 5 mm, (c) and depth 2 mm.

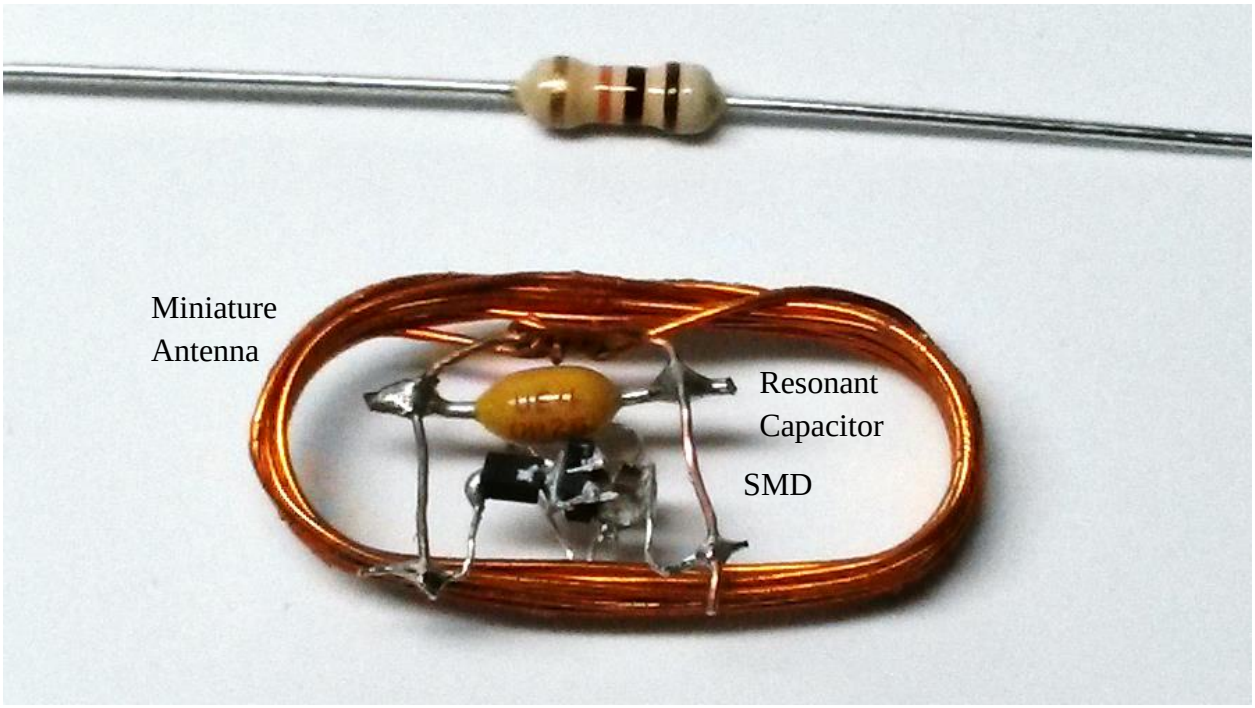

Figure 4.5. SMD device soldered onto LC circuit using miniature antenna.

4.3. Tissue Selection

For this experiment it was important to replicate human nerves as much as possible. All vertebrates have similar nerve structure. Organisms with well-developed nervous systems however, have compound nerves which consist of bundles of different types of nerve fibers which reach threshold for action potentials under slightly different conditions. These nerves have characteristic compound action potentials. Per suggestion of Dr. Caprio at LSU, professor of neurophysiology, a proper tissue sample that would be suitable for this experiment would be the frog sciatic nerve. This tissue lends itself well for our application for several reasons:

- There was an approved Institutional Animal Care and Use Committee (IACUC) protocol for the euthanasia of frogs for this specific tissue extraction, IACUC protocol #14059,

- The vertebrate physiology laboratory performed this type of extractions regularly for educational purposes,
- The data collection equipment to verify the compound action potentials was already in place at the vertebrate physiology laboratory,
- Frogs are inexpensive to purchase and maintain alive.

IACUC protocol approval typically requires 2-3 months of time. Thus, for the quick experimental turn-around and convenience, frog sciatic nerve was chosen as the *in vitro* tissue target for this experiment.

For the gastrocnemius (calf) muscle contraction experiment, the same euthanasia protocol is followed. A similar tissue extraction is followed as well, however, instead of completely removing the nerve tissue from the frog leg, a section is left attached at the knee. The leg bones are cut, and the gastrocnemius muscle left attached to the knee. It is then possible to cause muscle contractions by stimulating the sciatic nerve. The experimental conditions are now outlined.

4.4. Experimental Materials and Methods

For the experiment, the prototype was utilized as the stimulation signal generator. The AFG from the wireless resonance-coupled experiment was also used for this experiment. The AFG allows for "burst" signals to be easily generated, giving reliable power delivery to the device for specific time intervals. This feature allows the device to be operated at varying stimulation signal frequencies.

The tissue sample was collected according to the IACUC protocol #14059. A PowerLab 26T (ADInstruments, Dunedin, New Zealand) and computer provided by the vertebrate physiology laboratory were used for data collection. The PowerLab 26T has a capability of 100 ksps and excellent noise reduction, greatly increasing the fidelity and reliability of our results. The setup for the gastrocnemius muscle contraction experiment is shown in Figure 4.6. For control purposes, the PowerLab 26T has a built-in programmable neurostimulator used to elicit action potentials in target tissue during educational experiments. This stimulator was used as control for our experiment. The device electrodes were placed at about 7 mm distance from each other on the frog sciatic nerve in both experiments.

4.5. Device Operating as a Neurostimulator

The control and prototype elicited compound action potentials are shown in Figure 4.7 along with the normalized contraction force observed. The recorded compound action potentials did not show a significant difference in terms of amplitude when compared to the control. The threshold input voltage to elicit compound action potentials at 1 cm distance was 5.0 V. Increasing input voltage beyond this value at 1 cm distance increased the amount of fibers recruited by the stimulation, at 5.0 V only α fibers are recruited. These fibers run along the outer edge of the nerve bundle and are the first to elicit action potentials when there is a suitable stimulus. β fibers were recruited when using 5.5 V input power at 1 cm distance. These fibers show a much reduced action potential

amplitude and appear in the compound action potential measurement with a small delay. The lower action potential amplitude due to these fibers is due to the fact that it occurs deeper inside the nerve. The small signal at the left of Figure 4.7b is known as a stimulation artifact, and is due to the dispersion of current through the surface of the tissue and into the measuring electrodes. This artifact is normal and expected during these experiments. Muscle contraction results showed a difference in amplitude of about 15% between device-generated contraction and the control. This difference is due primarily to the fact that the muscle tissue utilized in the experiment was slowly dying. The control data was collected on fresh tissue less than 20 minutes after dissection, while the successful muscle contraction data was collected approximately 3 hours after dissection. The muscle exhibited fatigue as well, showing a greater amplitude during the first 2-3 contractions, and then a smaller contraction force thereafter, this effect can be seen in Figure 4.8.

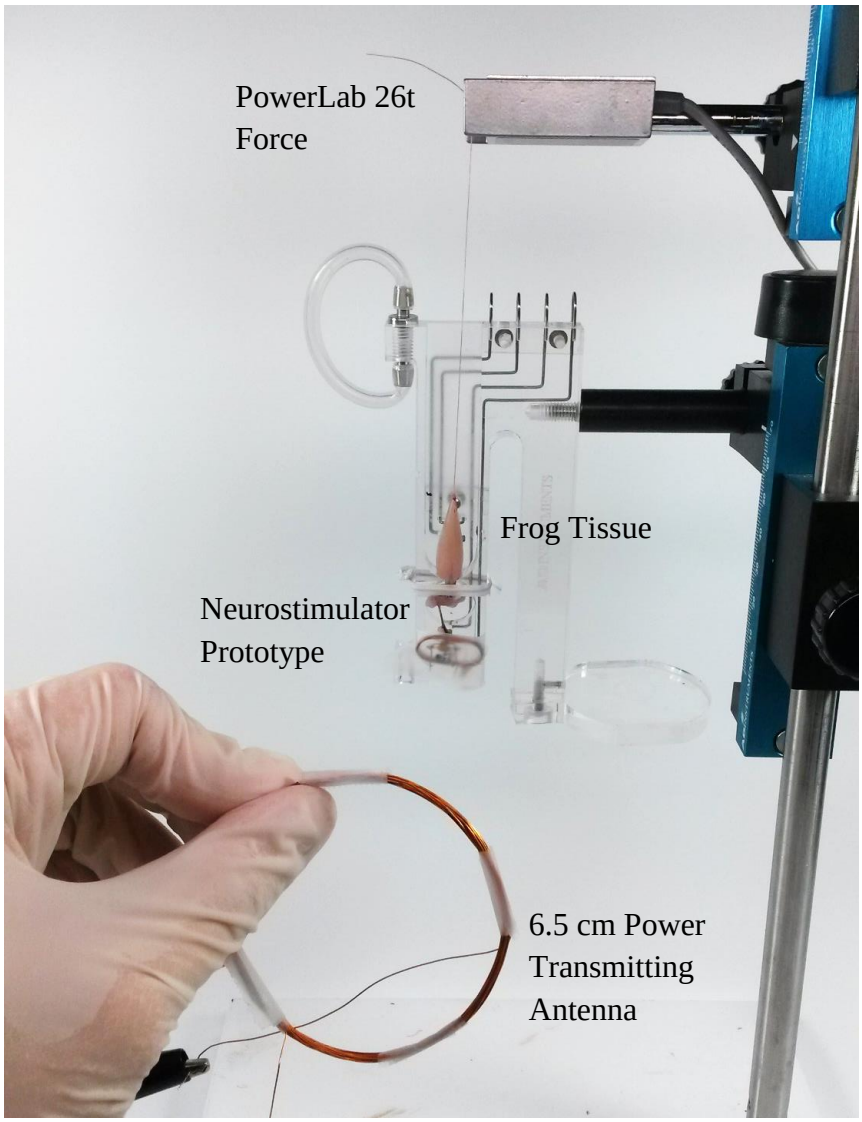

Figure 4.6. Setup for muscle contraction data collection showing power delivery antenna, prototype connected to frog sciatic nerve and gastrocnemius muscle, and force transducer feeding data to PowerLab 26t.

4.6. Summary and Discussion

The goal of this chapter was to outline the miniaturization process that was performed on the neurostimulator design presented in Chapter 3, and show proper neurostimulator operation *in vitro*. The importance of using the antenna as the largest component is discussed. Since this device is meant to be implantable and use wireless power, it makes sense to design the antenna as large as possible in order to increase the amount of power absorbed through wireless transmission. Taking antenna size into account, the miniature design was centered on using the antenna as support and housing for the neurostimulator circuit components. This unique approach allows maximizing the amount of power delivered, while minimizing the device footprint. The finished miniature device occupied approximately 1 cm^3, which is not much larger than a typical vitamin pill. The experiments performed on frog sciatic nerve and gastrocnemius muscle demonstrate the capability of the proposed circuit to operate as designed. Compound action potential were successfully measured at the frog sciatic nerve. Action potentials from recruited α and β fibers were shown, and they are identical to action potentials elicited by the control. There was successful muscle contraction caused by stimulation of the frog sciatic nerve. The contraction force was shown to be similar to the control however, it was smaller in amplitude since the experiments were performed on the same harvested tissue with 4 hours of difference. Harvested muscle tissue is dying over time, causing the contraction force to decrease as well. The "burst" feature of the AFG also demonstrated the capability of the device to vary the stimulation signal frequency, however, further experimentation must be performed to elucidate the maximum stimulation frequency limit. These results demonstrate the device is able to operate properly as a wireless, small-sized, neurostimulator.

The results from these experiments can be improved by performing a characterization on the neurostimulator device performance according to distance from the transmitting antenna and electrode placement. Finding the optimum electrode placement is key to improving the device efficiency. The maximum operating distance from the transmitting antenna should also be found. Improving the wireless power delivery system should yield greater reliability and flexibility for this neurostimulator design. Further miniaturization of the device should also be approached as further work in this project. *In vivo* experiments with recovery of motor function should be the next experimental target. The following section concludes the thesis and proposes suggestions for future work.

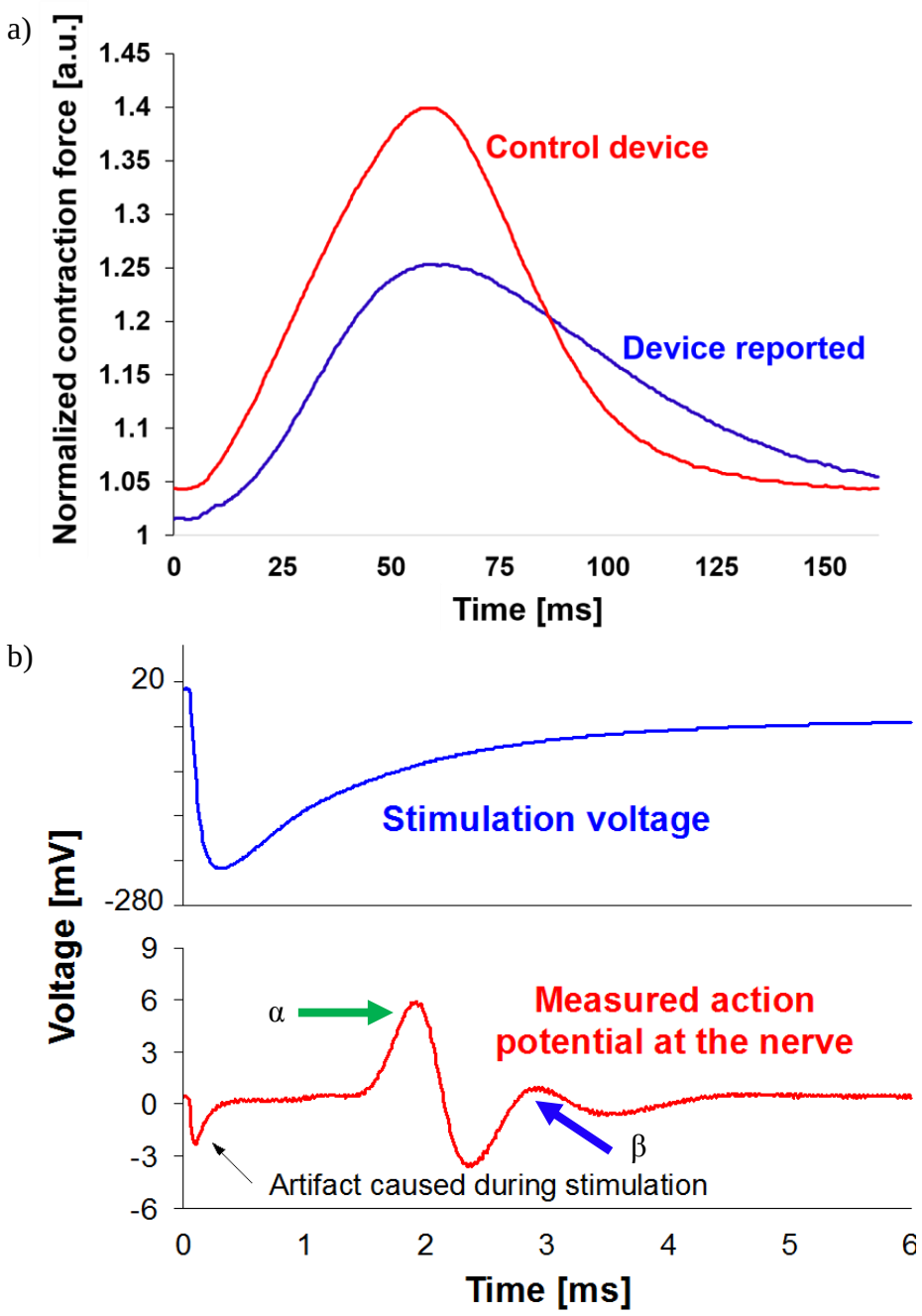

Figure 4.7. Average compound action potential and contraction force data: (a) average recorded gastrocnemius muscle contraction force from built-in neurostimulator in PowerLab 26t (red) and prototype (blue) and (b) red - Compound action potential, green arrow shows α fibers response, and blue arrow shows β fibers response.

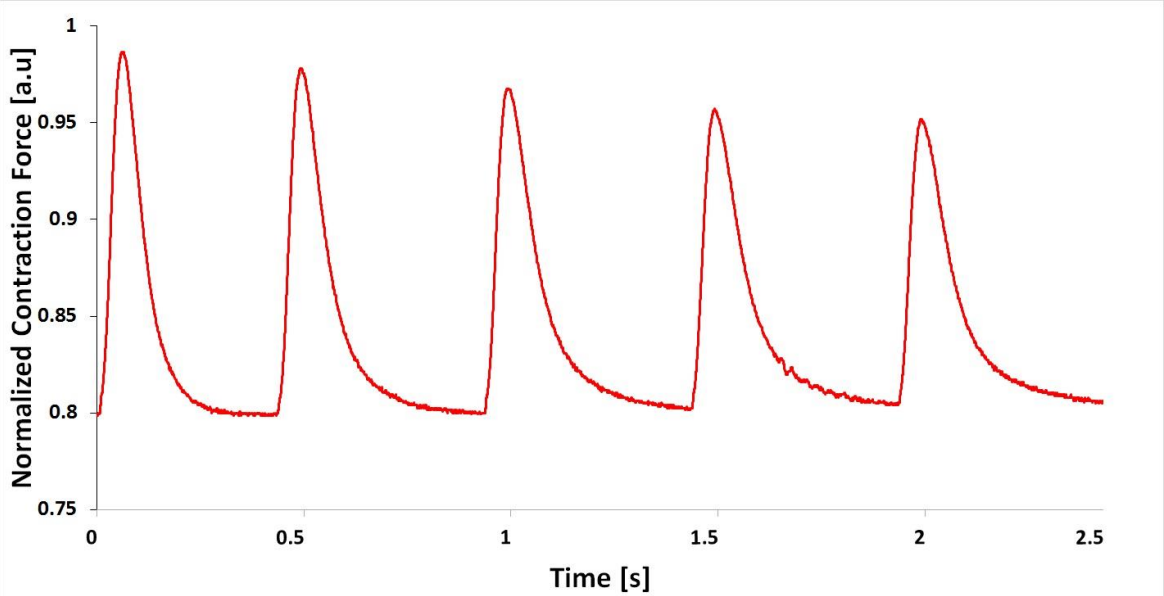

Figure 4.8. Fatigue in muscles shown by the periodic decrease in muscle contraction force. The force amplitude settled after this initial decrease with no change over 20 contractions.

CHAPTER 5. CONCLUSIONS AND FUTURE WORK

This thesis work outlined the design, characterization, and demonstration of a novel neurostimulator circuit that is intended to solve various current issues with state-of-the-art devices. First an introduction and motivation for the work was presented, followed by an overview of the thesis. A literature review was then presented which begins by providing a physiological description of the neuron, which is the target tissue for neurostimulators. The review then proceeded to summarize neural interface technology and its applications. Current neurostimulator state-of-the-art was presented and discussed. A table was presented which summarizes various performance metrics of the discussed neurostimulators.

The reasoning behind the design of a novel neurostimulator circuit was presented in Chapter 3. The design parameters involved in neurostimulator devices are described. The thesis work was focused on defining the output signal circuitry. The rationale behind this was that the neurostimulator circuitry defines the power deliver system, device size, and interface mechanisms, thus defining the majority of the parameters in the design. An outline of advantages and disadvantages of current neurostimulators was shown, and the derived solution requirements are discussed. The design of the neurostimulator circuit was presented and discussed. The circuit was designed to solve problems related to neurostimulator size, wireless capability, and control schemes. The stimulation circuitry was based off a modified capacitor-based stimulation scheme, and uses 2 RC circuits to provide the potential difference for a stimulation signal. The design was characterized, and the stimulation signal duration was shown to have a linear trend with respect to the capacitance of the RC circuits. The output signal voltage was shown to have a logarithmic trend, due to the fact that the output voltage was defined by the potential difference between two RC circuits. The chapter then shows a wireless resonance-coupled multichannel power delivery demonstration of the device. This demonstration shows the feasibility of the device to operate with wireless power.

This section could be improved by optimizing the circuit analytical equations. The presented analysis holds well for when the capacitors are discharging, but a suitable analytical solution has not been found for the charging case. Further work that characterizes the amount of charge delivered by the device according to various design parameters should also be performed. The circuit design should also be optimized, as there are indications that removing the rectifying diode would reduce the power consumption of the circuit while yielding the same performance. The wireless power delivery system requires optimization and characterization, such as determining the Q-factor, coupling coefficient, and power transmission efficiency of the antennas. An accurate power analysis should also be performed to allow easier design of the power transmission system.

Chapter 4 then continues to demonstrate the features of the device by describing the miniaturization process of the device and *in vitro* experiments. The device was miniaturized by using a small antenna with 10 x 20 x 3 mm dimensions as the housing and support structure for a custom-built SMD implementation of the device. The total volume occupied by the miniaturized

device was found to be approximately 1 cm^3, comparable to a typical vitamin pill. This unique approach allowed minimizing the device size while maximizing the area of the antenna. Results were shown for experiments conducted on frog sciatic nerve and gastrocnemius muscle. The neurostimulator device was shown to successfully elicit compound action potentials similar to the action potentials elicited by the control. α and β fibers were shown to be recruited by the neurostimulator. The neurostimulator device was then shown to successfully cause muscle contractions in the frog gastrocnemius muscle through stimulation of the frog sciatic nerve. There was an amplitude difference of about 15% between the control and neurostimulator. This difference was due to the fact that the two experiments were conducted on the same tissue, but separated by 4 hours. Muscle tissue died during this time, reducing the maximum contraction force that could be measured. A reduction in maximum contraction force was also shown to be a result of muscle fatigue, where the peak contraction force would decay periodically during stimulation until settling down. The device was successfully shown to operate as a neurostimulator in a miniature implementation.

The experiments in Chapter 4 can be improved by determining the maximum operating distance of the device with a given wireless power delivery system. Electrode placement can also be optimized, since this was not a parameter in the experiments conducted. Electrode placement can improve the efficiency of the device. The device should also be further miniaturized, with smaller components or an IC implementation. A more efficient antenna design should allow the device to be further miniaturized. *In vivo* experiments are the logical next step, and they should be focused on the restoration of motor control in injured animals such as rats.

This thesis demonstrated a novel neurostimulator design that solves current issues in the field. The design was characterized and successfully demonstrated to operate in a miniature wireless fashion with passive control. The device was shown to operate as a neurostimulator that successfully elicited compound action potentials in the frog sciatic nerve, and caused muscle contractions in the frog gastrocnemius muscle. Future optimizations related to the wireless power delivery system, circuit design, and miniaturization will allow the device to be used as an important tool in neural interfaces systems which require application-specific neurostimulators.

REFERENCES

[1] W. M. Grill, S. E. Norman, and R. V. Bellamkonda, "Implanted Neural Interfaces: Biochallenges and Engineered Solutions," *Annual Review of Biomedical Engineering,* vol. 11, pp. 1-23, 2009.

[2] A. M. Aravanis, L. Wang, F. Zhang, L. A. Meltzer, M. Z. Mogri, M. B. Schneider, *et al.*, "An optical neural interface: in vivo control of rodent motor cortex with integrated fiberoptic and optogenetic technology.," *Journal of Neural Engineering,* vol. 4, pp. S143-S156, 2007.

[3] N. Z. Mehenti, H. A. Fishman, and S. F. Bent, "A model neural interface based on functional chemical stimulation," *Biomedical Microdevices,* vol. 9, pp. 579-587, 2007.

[4] D. Warren, E. Fernandez, and R. Normann, "High-resolution two-dimensional spatial mapping of cat striate cortex using a 100-microelectrode array," *Neuroscience,* vol. 105, pp. 19-31, 2001.

[5] G. Baaken, M. Sondermann, C. Schlemmer, J. Rühe, and J. C. Behrends, "Planar microelectrode-cavity array for high-resolution and parallel electrical recording of membrane ionic currents," *Lab on a Chip,* vol. 8, pp. 938-944, 2008.

[6] N. G. Hatsopoulos and J. P. Donoghue, "The Science of Neural Interface Systems," *Annual Review of Neuroscience,* vol. 32, pp. 249-266, 2009.

[7] A. E. Schultz and T. A. Kuiken, "Neural Interfaces for Control of Upper Limb Prostheses: The State of the Art and Future Possibilities," *Physical Medicine and Rehabilitation,* vol. 3, pp. 55-67, 2011.

[8] S. Kim, K. Zoschke, M. Klein, D. Black, K. Buschick, M. Toepper, *et al.*, "Switchable polymer-based thin film coils as a power module for wireless neural interfaces," *Sensors and Actuators A: Physical,* vol. 136, pp. 467-474, 2007.

[9] M. A. L. Nicolelis, "Brain-machine interfaces to restore motor function and probe neural circuits," *Nature Reviews Neuroscience,* vol. 4, pp. 417-422, 2003.

[10] N. A. Campbell and J. B. Reece, "Biology," B. Wilbur, Ed., 8 ed San Francisco, CA: Pearson Education Inc., 2009, p. 16.

[11] T. Sasaki, N. Matsuki, and Y. Ikegaya, "Action-Potential Modulation During Axonal Conduction," *Science,* vol. 331, pp. 599-602, 2011.

[12] M. Velliste, S. Perel, M. C. Spalding, A. S. Whitford, and A. B. Schwartz, "Cortical control of a prosthetic arm for self-feeding," *Nature,* vol. 453, pp. 1098-1101, 2008.

[13] I. Saunders and S. Vijayakumar, "The role of feed-forward and feedback processes for closed-loop prosthesis control," *J Neuroeng Rehabil,* vol. 8, pp. 1-12, 2011.

[14] C. A. Angeli, V. R. Edgerton, Y. P. Gerasimenko, and S. J. Harkema, "Altering spinal cord excitability enables voluntary movements after chronic complete paralysis in humans," *Brain,* April 8, 2014 2014.

[15] D. R. Kipke, W. Shain, G. Buzsaki, E. Fetz, J. M. Henderson, J. F. Hetke, *et al.*, "Advanced Neurotechnologies for Chronic Neural Interfaces: New Horizons and Clinical Opportunities," *The Journal of Neuroscience,* vol. 46, pp. 11830-11838, 2008.

[16] J. M. Anderson, "Biological Responses to Materials," *Annual Review of Materials Research,* vol. 31, pp. 81-110, 2001.

[17] I. R. Minev, P. Musienko, A. Hirsch, Q. Barraud, N. Wenger, E. M. Moraud, *et al.*, "Electronic dura mater for long-term multimodal neural interfaces," *Science,* vol. 347, pp. 159-163, January 9, 2015 2015.

[18] J. Liu, H. Singh, and P. F. White, "Electroencephalogram bispectral analysis predicts the depth of midazolam-induced sedation," *Anesthesiology,* vol. 84, pp. 64-69, 1996.

[19] P. Kligfield, L. S. Gettes, J. J. Bailey, R. Childers, B. J. Deal, E. W. Hancock, *et al.*, "Recommendations for the standardization and interpretation of the electrocardiogram: part I: the electrocardiogram and its technology a scientific statement from the American Heart Association Electrocardiography and Arrhythmias Committee, Council on Clinical Cardiology; the American College of Cardiology Foundation; and the Heart Rhythm Society endorsed by the International Society for Computerized Electrocardiology," *Journal of the American College of Cardiology,* vol. 49, pp. 1109-1127, 2007.

[20] J-U. Meyer, M. Schuttler, H. Thielecke, and T. Stieglitz, "Biomedical Microdevices for Neural Interfaces," in *First Annual International IEEE-EMBS Special Topic Conference on Microtechnologies in Medicine and Biology*, Lyon, France, 2000, pp. 447-453.

[21] E. M. Maynard, C. T. Nordhausen, and R. A. Normann, "The Utah intracortical electrode array: a recording structure for potential brain-computer interfaces," *Electroencephalography and clinical neurophysiology,* vol. 102, pp. 228-239, 1997.

[22] K. Yoshida, D. Pellinen, D. Pivin, P. Rousche, and D. Kipke, "Development of the thin-film longitudinal intrafascicular electrode," in *Proceedings of the fifth Annual Conf. of the IFESS*, 2000, pp. 279-284.

[23] X. Navarro, S. Calvet, F. Rodriguez, T. Stieglitz, C. Blau, M. Buti, *et al.*, "Stimulation and recording from regenerated peripheral nerves through polyimide sieve electrodes," *Journal of the peripheral nervous system: JPNS,* vol. 3, pp. 91-101, 1997.

[24] S. T. Retterer, K. L. Smith, C. S. Bjornsson, K. B. Neeves, A. J. H. Spence, J. N. Turner, *et al.*, "Model Neural Prostheses With Integrated Microfluidics: A Potential Intervention Strategy for Controlling Reactive Cell and Tissue Responses," *IEEE Transactions on Biomedical Engineering,* vol. 51, pp. 2063-2072, 2004.

[25] A. M. J. P. Donoghue, M.Black, L. R. Hochberg, "Assistive technology and robotic control using motor cortex ensemble-based neural interface systems in humans with tetraplegia," *Journal of Phisiology,* vol. 3, pp. 603-611, 2007.

[26] P. Dario, P. Garzella, M. Toro, S. Micera, M.Alavi, U. Meyer, *et al.*, "Neural Interfaces for Regenerated Nerve Stimulation and Recording," *IEEE Transactions on Rehabilitation Engineering,* vol. 6, pp. 353-363, 1998.

[27] T. Tokuda, H. Kimura, T. Miyatani, Y. Maezawa, T. Kobayashi, T. Noda, *et al.*, "CMOS on-chip bio-imaging sensor with integrated micro light source array for optogenetics," *Electronics letters,* vol. 48, pp. 312-314, 2012.

[28] M. Schwaerzle, P. Elmlinger, O. Paul, and P. Ruther, "Miniaturized tool for optogenetics based on an LED and an optical fiber interfaced by a silicon housing," in *Engineering in Medicine and Biology Society (EMBC), 2014 36th Annual International Conference of the IEEE*, 2014, pp. 5252-5255.

[29] T. K. Whitehurst, J. H. Schulman, K. N. Jaax, and R. Carbumaru, "The Bion Microstimulator and its Clinical Applications," in *Implantable Neural Prostheses*, D. D. Zhou and E. Greenbaum, Eds., ed: Springer US, 2009, p. 22.

[30] P. J. Larson and B. C. Towe, "Miniature ultrasonically powered wireless nerve cuff stimulator," in *Neural Engineering (NER), 2011 5th International IEEE/EMBS Conference on*, 2011, pp. 265-268.

[31] S. Rehman and A. Kamboh, "A CMOS Micro-power and Area Efficient Neural Recording and Stimulation Front-End for Biomedical Applications," *Circuits, Systems, and Signal Processing*, pp. 1-22, 2014/12/02 2014.

[32] C. Seok, H. Kim, S. Im, H. Song, K. Lim, Y.-S. Goo, *et al.*, "A 16-channel Neural Stimulator IC with DAC Sharing Scheme for Artificial Retinal Prostheses," *JOURNAL OF SEMICONDUCTOR TECHNOLOGY AND SCIENCE,* vol. 14, p. 659, 2014.

[33] C. Sung-Hoon, X. Ning, L. Cauller, W. Rosellini, and L. Jeong-Bong, "A SU-8-Based Fully Integrated Biocompatible Inductively Powered Wireless Neurostimulator," *Microelectromechanical Systems, Journal of,* vol. 22, pp. 170-176, 2013.

[34] J. Vidal and M. Ghovanloo, "Towards a switched-capacitor based stimulator for efficient deep-brain stimulation," in *Engineering in Medicine and Biology Society (EMBC), 2010 Annual International Conference of the IEEE*, 2010, pp. 2927-2930.

[35] A. J. Yeh, J. S. Ho, Y. Tanabe, E. Neofytou, R. E. Beygui, and A. S. Y. Poon, "Wirelessly powering miniature implants for optogenetic stimulation," *Applied Physics Letters,* vol. 103, pp. 163701-163701-4, 2013.

[36] K. Y. Kwon, H.-M. Lee, M. Ghovanloo, A. Weber, and W. Li, "A wireless slanted optrode array with integrated micro leds for optogenetics," in *Micro Electro Mechanical Systems (MEMS), 2014 IEEE 27th International Conference on*, 2014, pp. 813-816.

[37] M. A. Rossi, V. Go, T. Murphy, Q. Fu, J. Morizio, and H. H. Yin, "A wirelessly controlled implantable LED system for deep brain optogenetic stimulation," *Frontiers in Integrative Neuroscience,* vol. 9, p. 8, 2015.

[38] T. J. Foutz and C. C. McIntyre, "Evaluation of novel stimulus waveforms for deep brain stimulation," *Journal of neural engineering,* vol. 7, p. 066008, 2010.

[39] A. S. Poon, S. O'Driscoll, and T. H. Meng, "Optimal frequency for wireless power transmission into dispersive tissue," *Antennas and Propagation, IEEE Transactions on,* vol. 58, pp. 1739-1750, 2010.

[40] M. Klemm and G. Troester, "EM energy absorption in the human body tissues due to UWB antennas," *Progress In Electromagnetics Research,* vol. 62, pp. 261-280, 2006.

[41] M. A. Jensen and Y. Rahmat-Samii, "EM interaction of handset antennas and a human in personal communications," *Proceedings of the IEEE,* vol. 83, pp. 7-17, 1995.

[42] W. Zaraska, P. Thor, M. Lipiński, M. Cież, W. Grzesiak, J. Początek, *et al.*, "Design and fabrication of neurostimulator implants—selected problems," *Microelectronics reliability,* vol. 45, pp. 1930-1934, 2005.

[43] W. Liu, K. Vichienchom, M. Clements, S. C. DeMarco, C. Hughes, E. McGucken, *et al.*, "A neuro-stimulus chip with telemetry unit for retinal prosthetic device," *Solid-State Circuits, IEEE Journal of,* vol. 35, pp. 1487-1497, 2000.

[44] J. C. Lilly, J. R. Hughes, E. C. Alvord Jr, and T. W. Galkin, "Brief, noninjurious electric waveform for stimulation of the brain," *Science,* 1955.

[45] K. H. Polasek, H. A. Hoyen, M. W. Keith, R. F. Kirsch, and D. J. Tyler, "Stimulation Stability and Selectivity of Chronically Implanted Multicontact Nerve Cuff Electrodes in the Human Upper Extremity," *Neural Systems and Rehabilitation Engineering, IEEE Transactions on,* vol. 17, pp. 428-437, 2009.

[46] K. H. Polasek, H. A. Hoyen, M. W. Keith, and D. J. Tyler, "Human Nerve Stimulation Thresholds and Selectivity Using a Multi-contact Nerve Cuff Electrode," *Neural Systems and Rehabilitation Engineering, IEEE Transactions on,* vol. 15, pp. 76-82, 2007.

[47] J. A. Parodi, E. A. Austin, and J.-W. Choi, "Neural Stimulator," United States Patent, 2014.

[48] B. L. Cannon, J. F. Hoburg, D. D. Stancil, and S. C. Goldstein, "Magnetic resonant coupling as a potential means for wireless power transfer to multiple small receivers," *Power Electronics, IEEE Transactions on,* vol. 24, pp. 1819-1825, 2009.

VITA

Jose Aquiles Parodi Amaya is an electrical engineer from Honduras. He was born into a family with one other sibling. His parents are engineers as well, and his brother is an anesthesiologist. He came to Louisiana State University in 2009 and has loved it ever since. Aquiles Parodi engaged in many organizations during his undergraduate degree, becoming a member of the rowing team, ballroom dance club, and acting as Director of Fusion the Honors College Literary Magazine during his senior year. He also graduated with College Honors from the Honors College. Now, he enjoys his time developing new biotechnology in the BioMEMS laboratory.